TAMPEREEN TEKNILLINEN YLIOPISTO
TAMPERE UNIVERSITY OF TECHNOLOGY

Jari Keskinen

Supercapacitors on Flexible Substrates for Energy Autonomous Electronics

Julkaisu 1562 • Publication 1562

Tampere 2018

Tampereen teknillinen yliopisto. Julkaisu 1562
Tampere University of Technology. Publication 1562

Jari Keskinen

Supercapacitors on Flexible Substrates for Energy Autonomous Electronics

Thesis for the degree of Doctor of Science in Technology to be presented with due permission for public examination and criticism in Tietotalo Building, Auditorium TB109, at Tampere University of Technology, on the 28th of September 2018, at 12 noon.

Tampereen teknillinen yliopisto - Tampere University of Technology
Tampere 2018

Doctoral candidate:
Jari Keskinen, Lic.Sci. (Tech.)
Laboratory of Electronics and Communications Engineering
Computing and Electrical Engineering
Tampere University of Technology
Finland

Supervisor:
Donald Lupo, Prof.
Laboratory of Electronics and Communications Engineering
Computing and Electrical Engineering
Tampere University of Technology
Finland

Pre-examiners:
Kai Vuorilehto
Adj. Prof.
Department of Chemistry
Aalto University
Finland
Director R&D
EAS Germany

Edgar Dörsam, Prof. Dr.-Ing.
Institute of Printing Science and Technology
Technische Universität Darmstadt
Germany

Opponent:
Xavier Crispin, Prof.
Laboratory of Organic Electronics
Linköping University
Sweden

ISBN 978-952-15-4180-3 (printed)
ISBN 978-952-15-4197-1 (PDF)
ISSN 1459-2045

Abstract

Electrical energy storage facilitates the use of electrical devices also when there is no full-time external energy source available. Electrical energy can be stored chemically as in batteries or in electric field as in capacitors. Supercapacitors are electrochemical cells in which energy is stored in electric field in the interface between electrode surface and electrolyte. Typically supercapacitors have higher power density but lower energy density than batteries. In general, supercapacitors have longer lifetime and they can be used in a wide temperature range.

The goal of the research reported in this thesis was to study and develop small, flexible, environmentally friendly supercapacitors for *e.g.* Internet of Things or wireless sensor network applications, with emphasis on inexpensive materials. A second focus of the research was on scalable solution based processes which are similar to mass printing making large-scale production feasible. A further goal was to avoid toxic materials in order to enable disposable or incinerable devices.

The supercapacitors were fabricated on paperboard or polymer substrates. Metal foils, silver ink and graphite ink were used as current collectors, activated carbon or polypyrrole as electrode material and paper as separator. Biopolymer chitosan was used as electrode binder and also demonstrated to work as a separator. In most experiments aqueous sodium chloride acted as electrolyte. Typically the area of the electrodes was 2 cm^2. A monolithic structure facilitating supercapacitor fabrication by a solution process method was developed.

The capacitance values of the supercapacitors were of the order of 0.1-0.5 F. Depending on the current collector material and dimensions, the equivalent series resistance ranged from below 1 Ω to above 30 Ω. Self-discharge properties for various types of supercapacitors were defined: still after 30 days over 50 % of the charged energy remained. Energy efficiency values were up to 96 %. These numerical values are adequate for energy storage components in practical application and thus show that the goals set for the research were reached.

Preface

This research work was carried out at VTT Technical Research Centre of Finland until 2014 and at the Laboratory of Electronics and Communications Engineering at Tampere University of Technology (TUT) from 2015. The projects in which the work was done were funded by the Finnish Funding Agency for Technology and Innovation (Tekes), industrial companies participating the projects, TUT and VTT. The financial support is gratefully acknowledged.

I would like to thank my supervisor, Prof. Donald Lupo, for his support and guidance throughout my work. I would also like to thank Suvi Lehtimäki and Sampo Tuukkanen for their work which has facilitated the success of supercapacitor development at TUT and made it possible for me to join the team. I also highly appreciate the cooperation made with the colleagues at VTT, especially Maria Smolander who made it possible to initiate the development of supercapacitors as a part of printed electronics research and Pertti Kauranen with whom the work with supercapacitors was started at VTT. I would also like to thank Mikael Bergelin for actively supporting the work by providing expertise in electrochemistry. I would also like to acknowledge especially the co-authors of the publications and also all my present and past co-workers at TUT and VTT as well as colleagues at Åbo Akademi, Aalto University and Uppsala University.

Finally, I thank my mother for her continuous encouragement in life as well as relatives and friends for being part of my journey. Most of all, I want to thank Maarit for her love and kind support.

Tampere 15.8.2018

Jari Keskinen

Contents

List of Symbols and Abbreviations

A / m^2	Area / Square meter
C / F	Capacitance / Farad
D / m	Distance / Meter
Q / C	Charge / Coulomb
P / W	Power / Watt
R / Ω	Resistance / Ohm
t / s / min / h	Time / Second / Minute / Hour
V / V	Voltage / Volt
W / J / kWh	Energy / Joule / Kilowatt hour
η / %	Efficiency / Percent

$\varepsilon_0 = 8.854 \times 10^{-12}\ \mathrm{F \cdot m^{-1}}$	Dielectric constant of vacuum
ε_r	Relative dielectric constant / Unitless

ACN	Acetonitrile
CDC	Carbide derived carbon
CNT	Carbon nanotube
CV	Cyclic voltammetry
EDLC	Electric double layer capacitor
EMIM	1-Ethyl-3-methylimidazolium
ESR	Equivalent series resistance
IHP	Inner Helmholtz plane
IoT	Internet of Things
OHP	Outer Helmholtz plane
PAni	Polyaniline
PC	Propylene carbonate
PE	Polyethylene
PEDOT	Poly(3,4-ethylenedioxythiophene)
PEO	Poly(ethylene oxide)
PET	Polyethylene terephthalate
PI	Polyimide
PP	Polypropylene
Ppy	Polypyrrole
PTFE	Polytetrafluoroethylene

PTh	Polythiophene
PVA	Polyvinyl alcohol
PVAc	Polyvinyl acetate
PVB	Polyvinyl butyral
PVDF	Polyvinylidene difluoride
Redox	Reduction and oxidation
RF	Radio frequency
R2R	Roll-to-roll
SEM	Scanning electron micrograph
SSA	Specific surface area
S2S	Sheet-to-sheet
$TEABF_4$	Tetraethylammonium tetrafluoroborate
UV	Ultraviolet
WSN	Wireless sensor network

List of Publications

I. Keskinen, J., Sivonen, E., Jussila, S., Bergelin, M., Johansson, M., Vaari, A. & Smolander, M. (2012). Printed supercapacitors on paperboard substrate, Electrochimica Acta, Vol.85, pp. 302–306.

II. Keskinen, J., Tuurala, S., Sjödin, M., Kiri, K., Nyholm, L, Flyktman, T., Strømme, M. & Smolander, M. (2015). Asymmetric and symmetric supercapacitors based on polypyrrole and activated carbon electrodes, Synthetic Metals, Vol. 203, pp. 192-199.

III. Keskinen, J., Lehtimäki, S., Dastpak, A., Tuukkanen, S., Flyktman, T. Kraft, T., Railanmaa, A. & Lupo, D. (2016). Architectural Modifications for Flexible Supercapacitor Performance Optimization, Electronic Materials Letters, Vol. 12 (6), pp. 795-803.

IV. Keskinen, J., Railanmaa, A. & Lupo, D. (2018). Monolithically prepared aqueous supercapacitors, Journal of Energy Storage, Vol. 16, pp. 243–249.

1 Introduction

Supercapacitors are energy storage devices able to provide high specific power. Compared to batteries their cycle life is typically longer and they can be used in wide temperature range. However, batteries have higher energy density. In practice supercapacitors are electrochemical cells including two electrodes and ionically conductive electrolyte. The electrodes are porous and isolated by a porous separator allowing ions to move in the electrolyte. (Conway 1999, Kötz and Carlen 2000) Commercial supercapacitors usually have metallic current collectors, activated carbon electrodes bound with polymer and liquid organic electrolyte. Aluminum cans are often used as encapsulation. (Azaïs 2013)

Small and inexpensive energy storage devices are needed in wireless sensor networks (WSN) and Internet of Things (IoT) applications. (Roselli et al. 2015, Lehtimäki 2017) Energy is needed in the sensors, when processing the obtained data and for sending the data to be processed outside the sensor. The energy can be harvested *e.g.* from light, motion, temperature difference or radio frequency (RF) signal. (Shaikh and Zeadally 2016) Since the energy source is not always available or relatively high power may be needed occasionally, it is essential to store the energy before using it. To facilitate the availability of high power the device should have relatively low output resistance. It would be beneficial that the energy storage devices could be easily recycled (Worrell and Reuter 2014, Veit and Bernandes 2013) or incinerated (Buykens 2013) with household waste. Thus using non-toxic materials is preferred. To keep the price of the components acceptable, both material and manufacturing costs should be low.

The aim of the research reported in this thesis was to meet the above listed requirements for small size energy source. Compared with conventional supercapacitors giving high specific power, our intended applications do not require high power and low output resistance. Obviously also in these applications long lifetime is often essential. The manufacturing processes and raw materials of supercapacitors were chosen to be feasible in mass-production, simultaneously keeping in mind that the materials and processes would be environmentally benign and inexpensive. The devices were made of solutions which can be applied using printing methods. Thus the manufacturing method allows high-volume industrial production using sheet-to-sheet (S2S) or roll-to-roll (R2R) processes. (Ganz et al. 2016) Concerning the safety of materials, the paperboard and polymer films used as substrates as well as metal foils are similar to the ones used *e.g.* for packaging consumer products such as food and beverages. Activated carbon and chitosan used in electrodes are non-toxic and the aqueous electrolytes contain sodium chloride or sodium nitrate, which can be found also in food products.

This thesis is based on the work reported in four peer-reviewed publications. In publication **I** supercapacitors made on paperboard have current collectors made of silver and graphite ink and activated carbon electrodes. Aqueous sodium chloride is used as electrolyte. Both single and series connected supercapacitors are reported. The mass decrease due to electrolyte evaporated and its effect on performance is discussed. Publication **II** presents the use of polypyrrole as electrode material. Aluminum-polymer laminate is used as substrate material and aqueous sodium nitrate as electrolyte. Both symmetric and asymmetric structures are reported. Electrical properties are measured using cyclic voltammetry and cycle life tests are presented. Publication **III** compares the properties of supercapacitors fabricated on paperboard and on polymer substrates having metallic coatings or foils to enhance electrical conductivity or improve barrier properties. Self-discharge and other electrical properties are reviewed. In publication **IV** a novel supercapacitor fabrication method based on solution processing and applying layers on top of each other is presented. The feasibility of solution processable separator layer made of chitosan is proved. The electrical properties are reported and compared with a supercapacitor made assembling two separate electrodes in face-to-face configuration.

Chapter 2 provides the background for the work by describing the techniques for the storage of electrical energy, essential electrical properties and materials typically used in supercapacitors. Printing and other solution processing methods are also briefly presented. The experimental details are described in chapter 3. Chapter 4 includes the results of the research. They are discussed from several points of view including substrate materials, current collector structure, electrode materials and the way how the supercapacitors can be fabricated.

Contribution of the author

The four publications have been made made in collaboration with other researchers. The contribution of the author is as follows:

Publication I: The author planned the experiments, fabricated the supercapacitors and characterized them. Eino Sivonen mixed the activated carbon ink. Discussions with Salme Jussila, Mikael Bergelin and Max Johansson were useful regarding supercapacitor design and characterization. Anu Vaari and Maria Smolander provided information of the biological fuel cell with which the supercapacitors were to be connected. The author wrote the first version of the manuscript. The manuscript was revised and improved with the co-authors.

Publication II : The author planned and made the samples and characterization in which sheet electrodes were used. Timo Flyktman made part of the laboratory work. Saara Tuurala and Kaisa Kiri made the experiments with printed polypyrrole electrodes. Uppsala University provided the sheet polypyrrole materials. The author wrote the first version of the manuscript together with Saara Tuurala who wrote the parts regarding printed polypyrrole electrodes and printed supercapacitor devices. The manuscript was revised and improved with the co-authors.

Publication III : The author planned the experiments, fabricated the supercapacitors and characterized them. Part of the laboratory work was made by Arman Dastpak and Timo Flyktman. Suvi Lehtimäki analyzed the self-discharge behaviour of the supercapacitors together with the author. The author wrote the first version of the manuscript. The manuscript was revised and improved with the co-authors.

Publication IV : The author planned the experiments, fabricated the supercapacitors and characterized the electrical properties. Anna Railanmaa made the SEM characterization. The author wrote the first version of the manuscript. The manuscript was revised and improved with the co-authors.

2 Background

2.1 Electrical energy storage in supercapacitors

Environmental issues require the replacement of fossil fuels with more sustainable alternatives. Renewable energy can be obtained from sun and wind, but since these are not available continuously, it is necessary to store energy. From an environmental point of view, using less energy is necessary, but also energy management can remarkably decrease the disadvantages. (Béguin 2013) Energy management means that energy is not used simultaneously with energy production but instead stored for later use.

For electrical energy storage the alternatives include batteries, superconducting electromagnets, capacitors and electrochemical capacitors, also called electric double layer capacitors, supercapacitors or ultracapacitors. (Conway 1999) Other forms of energy can be stored with methods such as pumped hydro, compressed air, flywheel and thermal systems. (Luo et al. 2015, Akinyele and Rayudu 2014, Sabihuddin et al. 2015) Conventional batteries can also be categorized as chemical energy storage but this group also includes systems such as fuel cells and flow batteries.

2.1.1 Supercapacitor compared with battery

Although the operation of supercapacitors seems quite similar to rechargeable batteries, i.e. the device can be charged by leading current to it and discharged by connecting a load to the electrodes, battery operation is based on chemical reduction and oxidation reactions (redox reactions, faradaic principle), in contrast to the electrostatic (non-faradaic) principle of supercapacitors. (Winter and Brodd 2004) The differences in specific energy and power between supercapacitors and batteries are largely due to the difference in operational principle. These parameters are often presented in a so called Ragone plot typically having specific energy (Wh/kg) on the x-axis and specific power (W/kg) on the y-axis. Figure 2.1 shows an example of a Ragone plot showing the properties of supercapacitors (electrochemical capacitors in the figure), various battery types and capacitors.

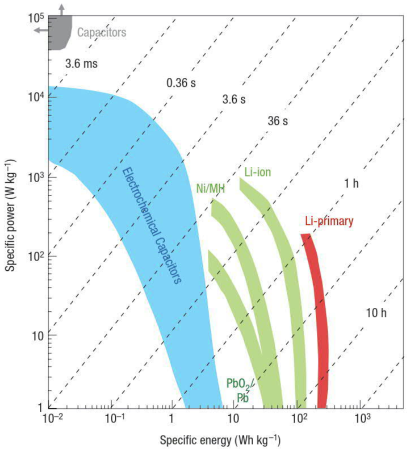

FIGURE 2.1. Ragone plot for electrical energy storing devices. The diagonal lines show time constants obtained by dividing the energy density by the power density. (Reprinted from (Simon and Gogotsi 2008) with permission.)

Table 2.1 shows typical values for supercapacitors, batteries and conventional electrolytic capacitors as a numerical presentation of the orders of magnitude shown in figure 2.1.

TABLE 2.1. Typical specific energy, specific power and time for discharge and charge for electrolytic capacitor, supercapacitor and battery. (Pandolfo and Hollenkamp 2006)

Characteristic	**Electrolytic capacitor**	**Supercapacitor**	**Battery**
Specific energy (Wh kg^{-1})	<0.1	1–10	10–100
Specific power (W kg^{-1})	$\gg$10000	500–10000	<1000
Discharge time	10^{-6} to 10^{-3} s	s to min	0.3–3 h
Charging time	10^{-6} to 10^{-3} s	s to min	1–5 h

2.1.2 Supercapacitor principle

In a capacitor, energy is stored in an electric field. A conventional capacitor consists of electrically conducting plates separated by an electrically insulating material. In a configuration like this the capacitance can be calculated from

$$C = \epsilon_o \, \epsilon_r \, \frac{A}{d} \tag{2.1}$$

where ϵ_o is the dielectric constant of vacuum, ϵ_r is the relative dielectric constant of the insulating material, A is the area of the conducting plates and d is the distance between the plates.

In an electrochemical capacitor, also called electric double layer capacitor (EDLC), supercapacitor or ultracapacitor, the energy is stored in the electric field at the interface between electrode and electrolyte as shown in figure 2.2. This operational principle facilitates much higher energy density in supercapacitors than achievable in conventional capacitors.

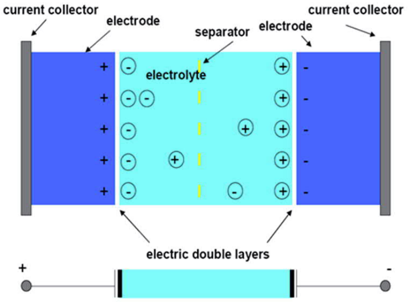

FIGURE 2.2. Operational principle of supercapacitor.

When a voltage difference is applied between the supercapacitor electrodes, the electric double layer is formed. The electronic charges on the surfaces of the electrodes cause the accumulation of negative and positive ions on the interfaces through Coulomb forces. (Yu et al. 2013) The thickness of the double layer is of the order of 0.5 – 1 nm, resulting in a double layer capacitance of 10 – 20 µF/cm^2. (Kötz and Carlen 2000)

There are many different theories on the basis of which the electric double layer is modelled. (Gonzalez et al. 2016, Yu et al. 2013, Conway 1999, Simon et al. 2013) Figure 2.3 illustrates the development starting from the simple Helmholtz model to more complicated Stern-Grahame model.

On the surface of the positively charged electrode the concentration of negative ions is increasing and the potential at each point behaves accordingly.

In the Helmholtz model it is assumed that negative charges accumulate at a constant distance (d) from the positive charges in the electrode. This model helps in understanding the interface but does not satisfactorily explain the physical phenomena. (Gonzalez et al. 2016)

Compared to the Helmholtz model, the Gouy-Chapman model allows the ions not to be at constant distance from the interface. It is also called diffuse model, since the ions in the electrolyte diffuse further from the interface. In the diffuse model it is assumed that ions are point charges and there are no practical limitations how near the interface the ions can move. (González et al. 2016)

The Stern model combines the Helmholtz and Gouy-Chapman models by including both the charges at a constant distance from the electrode and those in the diffuse layer. Grahame further improved the model by introducing separate inner and outer Helmholtz planes, marked with IHP and OHP in figure 2.3 (c). (Conway 1999) The reasoning for this is that the most common cations are smaller than common anions and thus keep their solvation shells.

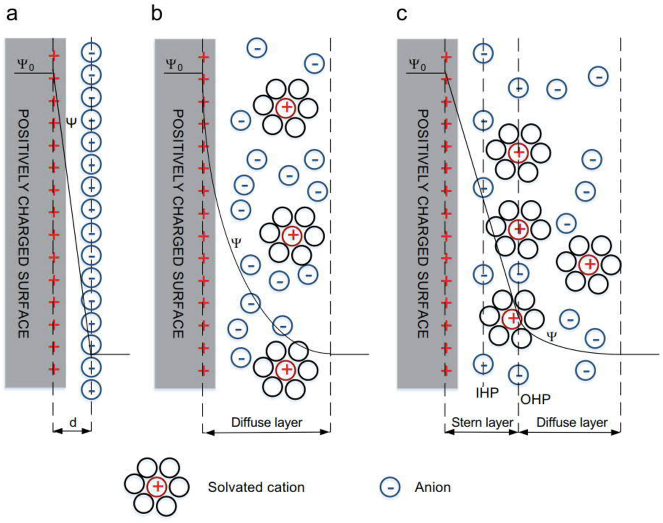

FIGURE 2.3. Models for electric double layer at the interface of electrode and electrolyte. (a) Helmholz model, (b) Gouy-Chapman model, (c) Stern-Grahame model. (Reprinted from (González et al. 2016) with permission.)

To achieve high capacitance it is necessary to have high electrode surface area. In practice this can be obtained by applying highly porous electrode materials. The electrolyte including the ions penetrates into the pores, thus generating high electrolyte-electrode interface area. Figure 2.4 shows the practical structure of a supercapacitor.

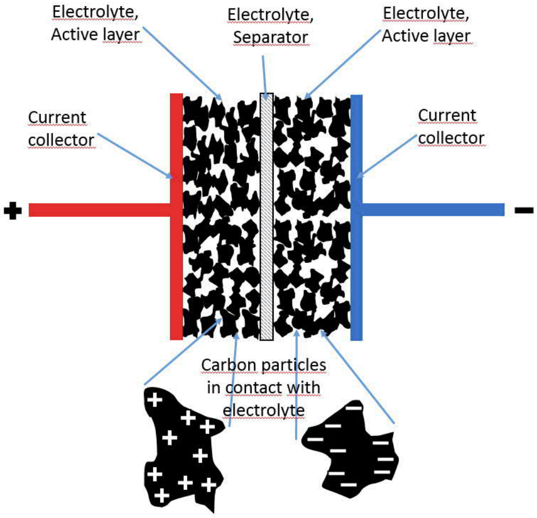

FIGURE 2.4. Practical structure of a supercapacitor. Adapted from (Kötz and Carlen 2000).

Since effectively there are two interfaces with electric double layer inside a supercapacitor, the total capacitance C can be calculated from the capacitances on the positive electrode and negative electrodes from the formula

$$C = \frac{C_1 \, C_2}{C_1 + C_2} \tag{2.2}$$

To avoid short-circuit between the electrodes it is necessary to use a porous separator made of electrically insulating material. The pores are necessary to facilitate the ion transport inside the electrolyte.

Figure 2.5 shows the classification and various structures used in supercapacitors. Typically the term supercapacitor refers to an energy storage device where two similar electrodes made of high-surface area carbon such as activated carbon (Marsh and Rodriguez-Reinoso 2006, Sevilla and Mokaya 2014, McDougall 1991), carbon nanotubes or graphene are used as positive and negative electrodes in an electrochemical cell. In this case the energy is stored in the electric double layer. The structure having similar positive and negative electrodes is called symmetric. In rechargeable batteries the structure is asymmetric, *e.g*. in lead-acid batteries the negative electrode is made of lead (Pb) and the positive electrode of lead oxide (PbO_2) or in lithium-ion batteries the reacting negative electrode material is lithiated graphite (LiC_6) and positive electrode material lithium metal oxide (*e.g*. $LiCoO_2$ or $LiFePO_4$). It is also possible to use metal oxides such as ruthenium oxide or manganese oxide or conducting polymers as electrodes of a supercapacitor. (Simon and Gogotsi 2008, Snook et al. 2011, Simon et al. 2014) Their electrical behavior is based on redox-reactions on the surface and inside the material. These redox reactions are fast and since the behavior of the devices is similar to that of capacitors, they are called pseudocapacitors. They can have higher specific energy storage capacity than supercapacitors with activated carbon electrodes. Intrinsically conducting polymers such as polyaniline or polypyrrole can be used on both electrodes or only on one electrode combined with another electrode consisting of activated carbon. A hybrid supercapacitor consists of an electrode based on the formation of electric double layer and of an electrode with pseudocapacitive or battery-type function. (González et al. 2016, Vangari et al. 2013) An example of these is a lithium-ion capacitor. (Smith et al.2013)

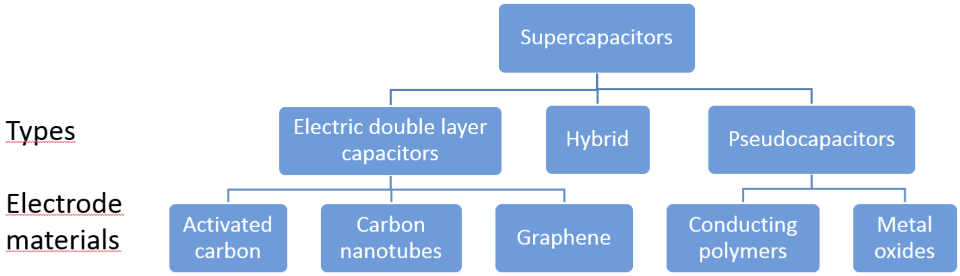

FIGURE 2.5. Supercapacitor types and electrode materials. (González et al. 2016) In this thesis supercapacitors based on activated carbon and on conducting polymers are reported.

2.1.3 Applications of supercapacitors

When manufacturing a storage system for electrical energy, the choice between supercapacitors and rechargeable batteries depends on the requirements set by the application. As can be concluded from figure 2.1, batteries are generally preferred when the specific energy is the most critical parameter. When there is a need for short-term power peaks, supercapacitors may be the best alternative. Beside high power, other properties favoring the use of supercapacitors are their wide temperature range (typically about -40 - +70 ^{o}C) (Xiong et al. 2015) and high cycle-life (millions vs thousands for batteries) (Pandolfo et al. 2013) compared to typical rechargeable batteries.

Obviously since different applications require energy capacity of varying size, the capacitance range available is very wide as shown in table 2.2 for commercially available supercapacitors. Supercapacitors are used when their properties are more suitable than those obtainable with conventional capacitors or batteries.

TABLE 2.2. Examples of commercial supercapacitor manufacturers and the capacitance and voltage range of their products. (Bussmann 2018, Ioxus 2018, LS Mtron 2018, Maxwell 2018, Murata 2018, Nippon Chemi-Con 2018, Panasonic 2018)

Company	**Capacitance range (F)**	**Voltage range (V)**
Bussmann	0.1 - 3400	2.5 - 5.5
Ioxus	1300 - 3150	2.7 – 2.85
LS Mtron	100 - 3400	2.7 – 3.0
Maxwell	1 - 3400	2.7 - 2.85
Murata	0.035 - 1	4.2 – 5.5
Nippon Chemi-Con	50 - 1400	2.5
Panasonic	0.1 - 100	2.1 – 5.5

Supercapacitors are used in memory protection or back-up power applications, especially due to their longer cycle life and improved safety compared to batteries. Because of their high specific power supercapacitors can complement battery systems when high output power is needed. In this way the battery lifetime can be enhanced and in some cases smaller and thus more inexpensive batteries can be used. In portable electronic devices with moderate energy requirement supercapacitors can act as a stand-alone power source. They can handle peak power events for positioning system, audio, wireless transmission, camera flash or video and supply power to facilitate battery change without shutting off the device. Supercapacitors can improve the electric power quality by removing voltage fluctuations and thus protecting electronic devices from damages. Since the time period of voltage disturbances is often relatively short, the limited energy content of a supercapacitor is not a problem. In hybrid vehicles supercapacitors can be used together with batteries, fuel cells or internal combustion engines to save energy or boost the performance. Renewable energy sources such as wind or solar power can not provide constant energy levels: thus to even the fluctuations an intermittent energy storage system is required. Especially when there is a need for relatively short time operation, excellent cycle lifetime or reliable operation also at low temperatures, supercapacitors can be expected to be the best solution. (Yu et al. 2013)

Supercapacitors are also potential energy storage components in Internet of Things (IoT) applications. IoT refers to objects connected to internet without human intermediation. IoT systems must have components for sensing and communication and the systems should be energy-autonomous and eco-friendly. (Roselli et al. 2015) A schematic of an Internet of Things device including these parts is shown in figure 2.6. One possibility towards eco-friendliness in powering the connected objects is replacing primary and secondary batteries with energy harvesting from light, electromagnetic radio frequency (RF) or kinetic energy. Since the energy is usually not available continuously, energy storage is necessary. This can be implemented using thin, flexible and non-toxic supercapacitors. (Lehtimäki et al. 2014, Pörhönen et al. 2014)

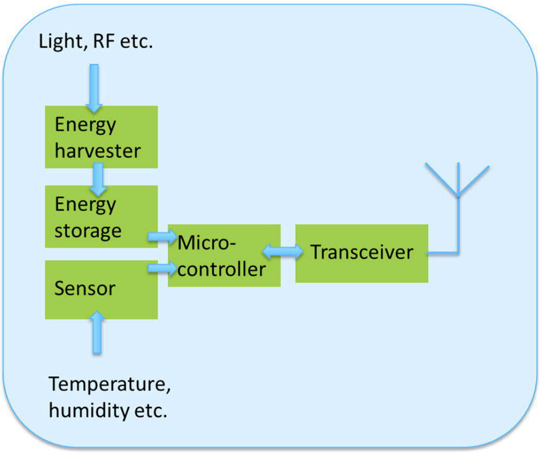

FIGURE 2.6. An autonomous wireless sensor device for IoT applications including parts for sensing, energy management, data processing and communications.

2.2 Properties of supercapacitors

2.2.1 Capacitance and charge

Capacitance (Conway 1999, Yu et al. 2013) is the ratio of charge (Q) on each electrode and voltage difference (V) across them according to

$$C = \frac{Q}{V} \tag{2.3}$$

The unit for capacitance is Farad (F). The charge (Alonso and Finn 1979) generated by constant current (I) during a time period (dt) is

$$dQ = I\,dt \tag{2.4}$$

Thus when a capacitor is charged or discharged with constant current, its capacitance can be calculated from the voltage change rate and current according to

$$C = \frac{I}{dV/dt} \tag{2.5}$$

Specific capacitance defines the capacitance related to mass or volume. It should be clearly expressed which mass or volume is used since the mass or volume may refer to one electrode, two electrodes or to the total mass or volume of the whole supercapacitor.

2.2.2 Voltage and energy

The potential distribution and equivalent circuit model of a supercapacitor is shown in figure 2.7. When voltage is applied, the potential difference is distributed at the interfaces between electrolyte and electrodes as well as inside the electrolyte (due to ionic resistance) and inside the electrodes and current collectors (due to electrical resistance). In principle, when the supercapacitor is disconnected i.e. it is neither charged nor discharged the potential differences are located only at the electrode-electrolyte interfaces.

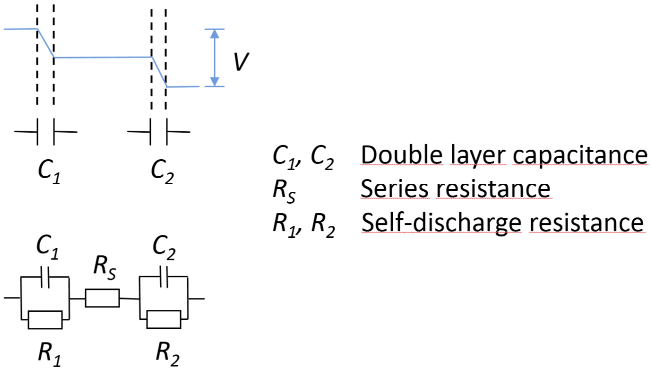

FIGURE 2.7. Potential distribution inside a supercapacitor and its equivalent circuit model. (Zhang and Zhao 2009)

The energy stored in a charged capacitor is

$$W = \frac{1}{2} C V^2 \tag{2.6}$$

where C is the capacitance of the capacitor and V is the voltage over it. (Kötz and Carlen 2000) Since the energy is proportional to the square of the voltage, maximizing the voltage can considerably increase the energy storage capacity. The maximum voltage of commercially available supercapacitors is often of the order of 2.5-2.8 V. (Zhong et al. 2015) This is due to the fact that the most commonly used electrolytes are organic compounds which would dissociate at higher voltages. In the case of water based electrolyte the potential window is around 1.23 V. (Zhong et al. 2015) In some commercially available single components the maximum voltage is about 5 V, which is achieved by connecting two separate cells using organic electrolyte in series inside the encapsulation.

Analogously to specific capacitance, energy can also be related to the mass or volume of the supercapacitor device to define specific energy or energy density.

2.2.3 Equivalent series resistance and power

The equivalent series resistance (ESR) of a supercapacitor consists of the resistance of current collectors and electrodes as well as of the ionic resistance of the electrolyte. The contact resistances in the interfaces between these layers or materials also contribute to the ESR. In the equivalent circuit model presented in Figure 2.7 the resistor R_s includes all these components of ESR.

The ESR affects especially the power available from the supercapacitor. The maximum power is (Kötz and Carlen 2000)

$$P = \frac{V^2}{4R} \tag{2.7}$$

where *V* is the voltage across the supercapacitor and *R* is the ESR. Thus in case the voltage is limited by the choice of electrolyte, ESR is the most critical parameter to maximize the output power. The ESR can be decreased by applying current collectors, electrodes and electrolyte with low resistivity. Optimized geometry of the supercapacitor is also essential. The paths of electrodes and ions can be made shorter and wider to optimize the ESR. Although the porous separator between the electrodes is made of insulating material, the structure of its pores has effect on the ionic resistance of the electrolyte layer. In a similar way, the pore structure of the electrodes contributes to the ionic resistance.

In the same way as specific energy, specific power or power density can be defined relative to supercapacitor mass or volume.

2.2.4 Self-discharge and leakage current

Self-discharge is the phenomenon which causes the voltage of a charged supercapacitor to decrease even when it is not electrically connected to a load. The reasons can be related to chemical reactions or physical processes. (Andreas 2015, Conway 1999, Conway et al. 1997, Niu et al. 2004) To keep supercapacitor voltage constant, a small current is needed to maintain the voltage. This current is called leakage current. There are several mechanisms to cause self-discharge:

1. Ohmic leakage between the electrodes
2. Overcharging beyond electrolyte solution decomposition potential
3. Parasitic Faradaic reactions
4. Charge redistribution

The Ohmic leakage is caused by a resistive pathway between the positive and negative electrode. This is due to a problem *e.g.* in constructing the supercapacitor or because of a mechanical failure. Overcharging beyond the electrolyte decomposition can be obviously avoided by keeping the voltage low enough, *e.g*. in case of aqueous electrolytes below the decomposition potential of water.

The parasitic Faradaic reactions are reduction and oxidation (redox) reactions on the electrode surface discharging the electrode. For instance, on the positive electrode the potential may be higher than the oxidation potential of impurity ions such as *e.g.* iron in solution on the electrode surface. (Andreas 2015) The oxidation of the impurities causes electrons to move across the double layer into the electrode surface, which further releases the anions from the double layer, decreasing the potential of the electrode. The reactions on the negative electrode are analogous and, for instance, the reduction of oxygen can discharge the negative electrode.

Charge redistribution causes a phenomenon which is similar to self-discharge but mainly relevant only for relatively short time periods. It is due to the time difference between charging different parts in the porous electrode structure. The outer part of the electrode charges more quickly than the surfaces located deep in the pores. When the charging is ended before it is completed, charges continue moving deeper into the material, which causes the voltage to decrease and is thus visible as self-discharge.

2.2.5 Efficiency

The efficiency of a supercapacitor tells what percentage of charged energy or charge can be recovered after charging the supercapacitor. Two types of efficiency are called energy efficiency and charge or Coulombic efficiency, respectively.

The properties affecting the efficiency values are ESR and leakage current. When charged or discharged, part of energy is lost in the series resistance. Thus minimizing the ESR is extremely important since, besides increasing the maximum power, it also reduces losses. Obviously the charge lost due to self-discharge is not available to produce current during supercapacitor discharge phase so, the self-discharge deteriorates both energy and charge efficiencies.

2.2.6 Temperature range

As already mentioned with respect to application potential, the temperature range of supercapacitors is typically wider than that of batteries. The range is mainly limited by the properties of the electrolyte. (Zhong et al. 2015) To enable ionic conductivity, the electrolyte may not prevent the ions to move, thus the solidification of an electrolyte sets the low temperature limit. At high temperature the electrolyte starts to boil or decompose, which increases the pressure inside the supercapacitor with destructive consequences.

An approximate temperature range for supercapacitors with aqueous electrolytes is from -10 to near + 100 ^{o}C, with organic electrolytes from -40 to +70 ^{o}C and with ionic liquid electrolytes from room temperature to over 100 ^{o}C. (Xiong et al. 2015)

2.2.7 Cycle life, calendar lifetime

The basic reason for the longevity of supercapacitors is that their operation does not require chemical or electrochemical reactions. When charging or discharging, ions and electrons move inside electrolyte and electrodes. Thus compared to batteries, dimensional changes due to electrochemical reactions do not take place and the materials are not exposed to mechanical deterioration in the same way.

Supercapacitors also deteriorate with time, though slowly, especially at high temperature and when high voltage is applied over them. (Bohlen et al.2007A, Bohlen et al. 2007B, Kötz et al. 2006) Although energy storage in supercapacitors is not based on Faradaic reactions, parasitic electrochemical reactions occur and can reduce the lifetime. Increasing temperature and voltage accelerate the ageing reactions exponentially. Typically the capacitance decreases and ESR increases with time. (Azaïs et al. 2007)

The processes leading to ageing are mainly side-reactions that lead to electrolyte loss, blocking of the pores in electrodes and generation of volatile side-products, which may result in gas bubble formation and thus pressure increase inside the supercapacitor. (He et al. 2016, Ratajczak et al. 2014) Surface functional groups and impurities (water in organic electrolyte, metals and *e.g*. oxygen) contained in the activated carbon electrodes are possible reasons for the deterioration of electrical properties. (Azaïs et al. 2007) The encapsulation of a supercapacitor may be an essential factor in determining the lifetime. Poor barrier properties against electrolyte evaporation or against oxygen penetration from air can result in fast degradation.

2.3 Supercapacitor materials

2.3.1 Electrodes

As already mentioned, activated carbon (Marsh and Rodriguez-Reinoso 2006, Sevilla and Mokaya 2014, McDougall 1991, White 2015) is the most commonly used electrode material in supercapacitors. From a microstructure point of view, activated carbon materials are assemblies of defective graphene layers. (Marsh and Rodriguez-Reinoso 2006) Activated carbon fulfills the basic requirements for the electrode material, having high specific surface area of the order of 1000-2500 m^2/g (Frackowiac et al. 2013), excellent chemical and thermal stability as well as good electrical conductivity. The structure of activated carbon is presented in figure 2.8. Besides, it can be made of relatively inexpensive raw materials and the manufacturing costs are low. (Yan et al. 2014, González et al. 2016, Simon and Gogotsi 2008) The raw material can be for instance coconut shell, wood, oil, coal or polymer. The activated carbon grades manufactured for supercapacitor application are mainly made of coconut shells. (Weinstein and Dash 2013) To synthesize activated carbon, the raw materials are first carbonized, i.e. heat treated in inert atmosphere and then activated *e.g*. in steam or carbon dioxide at high temperature to obtain the porous structure. To facilitate adequate electrical properties and long lifetime in supercapacitors, activated carbon needs to be pure enough. The ash content should be below 1 % and halogen and iron concentration below 100 ppm. (Weinstein and Dash 2014) The activation process increases specific surface area (SSA) and pore volume resulting in formation of micropores (<2 nm), mesopores (2-50 nm) and macropores (>50 nm). The double layer capacitance of activated carbon can be of the order of 150-300 F/g in aqueous electrolytes and 100-120 F/g in organic electrolytes. (Simon and Gogotsi 2008)

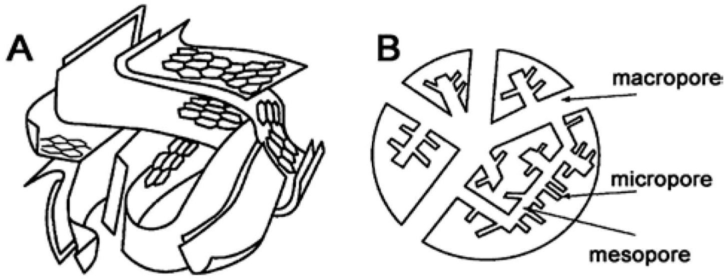

FIGURE 2.8. Schematic three-dimensional crystalline and two-dimensional pore structure of activated carbon. Reprinted from (Rodriguez-Reinoso 1998) with permission.)

The electric double layer models presented earlier (Figure 2.3) are valid for plane surfaces. Introducing a surface structure consisting of small pores makes the situation more complicated. Ion behavior in micropores (<2 nm) is yet not perfectly understood, but generally it is obvious that if the pores are too small the ions are not able to access there, thus the surface area inside the micropores may not increase the capacitance. (González et al. 2016, Barbieri et al. 2005)

The knowledge of the behavior of micropores contributing electric double layer capacitance was considerably increased by new findings related to pore sizes below 1 nm. (Chmiola et al. 2006, Frackowiac et al. 2013) They made experiments with activated carbon materials having well-defined micropore size distribution. The specific capacitance values were considerably higher than expected. It was suggested that the solvation shell of ions gets distorted, allowing the ions to pack nearer to each other and the electrode surface than expected earlier, resulting in clearly higher specific capacitance. Minimizing pore size may not be the optimal way to enhance supercapacitor performance, since larger pore size enhances the ion flow to and from the electrode-electrolyte interface, decreasing ion resistance. For optimization of the specific energy, small pore size is beneficial, whereas to maximize the power output larger pore size or short pore length are necessary. (Chmiola et al. 2006)

Activated carbon materials having sub-nanometer pore size can be made using carbide materials such as *e.g*. titanium carbide or silicon carbide as precursor. The manufacturing process includes etching the carbide in the presence of halogen at high temperature. In the case of TiC, chlorine gas reacts with TiC forming porous carbon and $TiCl_4$. (Simon and Gogotsi 2008) The pore structure of the carbon material can be optimized by reaction parameters. Carbon material made in this way is called carbide derived carbon (CDC).

The activated carbon used in supercapacitors is often in powder form, but also activated carbon cloth can be used. Both alternatives can reach approximately same SSA, but the cloth is typically more expensive. The price of commodity activated carbon is about $4/kg whereas due to enhanced requirements the supercapacitor grade activated carbon powder costs about $15 /kg. (Weinstein and Dash 2013) To improve the electrical conductivity of supercapacitor electrodes, a few percent of carbon black is often added to activated carbon. (Balducci and Schütter 2015, Azaïs 2013)

Carbon nanotubes (Endo et al. 2008) (CNT) are an interesting group of supercapacitor electrode materials. They have high electrical conductivity as well as excellent mechanical, chemical and thermal stability. (Yan et al. 2014, Endo et al. 2008) However, compared to activated carbon materials, they have lower specific surface area of below 600 m^2/g. Although the surface area is relatively moderate, electrolyte can access the surface more easily than the pores in activated carbon.

Untreated CNT electrodes have typically shown specific capacitance values clearly below 100 F/g. (Obreja 2014, Simon and Gogotsi 2008) By adding oxygen-rich groups on the CNT surface, over 100 F/g has been reached. (Simon and Gogotsi 2008) Oxygen plasma treatment has even resulted in about 440 F/g (Yan et al. 2014) by combining double-layer capacitance and redox pseudocapacitance. To achieve this kind of combination, there is also interest in fabricating composites combining CNTs and conducting polymers or metal oxides, in these cases the polymer contributes by giving pseudocapacitance. (González et al. 2016, Singh and Chandra 2015) CNTs are also a potential electrode alternative in flexible and light-weight supercapacitors. (Wang et al. 2016) Despite many advantages, some drawbacks should still be overcome to increase the commercial potential of CNT electrodes in supercapacitors. These include the limited SSA, purity issues and high production costs. (Yan et al.2014)

Graphene is a one-atom thick sheet consisting of carbon atoms. (González et al. 2016) Its SSA is 2630 m^2/g (Yan et al. 2014) and theoretical specific capacitance of 550 F/g (Kim et al. 2015). From a supercapacitor electrode application point of view it has similar properties to those of CNTs. It has high electrical conductivity, excellent mechanical properties and its surface is easily accessible to the electrolyte. (Kim et al. 2015) Maximum specific capacitances exceeding 200 F/g have been reported. (González et al. 2016, Yan et al. 2014) Supercapacitors with graphene electrodes often show irreversible capacity loss due to agglomeration or re-stacking of graphene sheets. Composites of graphene and metal oxides have been fabricated to avoid the re-stacking and to increase the available surface area. (González et al. 2016) Beside the re-stacking, also the challenges in large-scale synthesis of high-quality graphene have inhibited the commercial use of graphene in supercapacitor electrodes.

Applying conductive polymers in supercapacitor electrodes is intended to result in specific energy levels between those of carbon-based supercapacitors and batteries. (Snook et al. 2011, Bryan et al. 2016, Edberg et al. 2018) Typical conducting polymer materials in the electrodes include polyaniline (PAni), polypyrrole (PPy), polythiophene (PTh) and derivatives of polythiophene like PEDOT (poly(3,4-ethylenedioxythiophene). Table 2.3 shows theoretical and experimental specific capacitances of conducting polymers as well as some basic properties. The molecular weight is per unit monomer. The dopant level tells how many dopants there can be per polymer unit.

TABLE 2.3. Essential properties of conducting polymers in supercapacitor electrode application (Snook et al. 2011)

Conducting polymer	**Molecular weight (g/mol)**	**Dopant level**	**Potential range (V)**	**Theoretical specific capacitance (F/g)**	**Measured specific capacitance (F/g)**
PAni	93	0.5	0.7	750	240
Ppy	67	0.33	0.8	620	530
PTh	84	0.33	0.8	485	-
PEDOT	142	0.33	1.2	210	92

Conducting polymers are often used in combination with carbon nanotubes or inorganic battery electrode materials. The pseudocapacitance originating from the redox reactions can result to higher capacitance than achievable with carbon electrodes. In general, the resistivity of the conductive polymers is lower than that of typical battery materials, which potentially improves power density. Compared to activated carbon electrodes, the drawback is that conductive polymer electrodes have dimensional changes when charged or discharged leading to shorter cycle life, typically a few thousand cycles whereas carbon based electrodes can be cycled over 500 000 times.

Conducting polymers are conductive due to their conjugated bond system along the polymer backbone chain. They can be p-doped with anions when oxidized and n-doped with cations when reduced. When a supercapacitor has both electrodes made of conductive polymers it can be either symmetric or asymmetric. In the symmetric case it has the same p-dopable polymer in both electrodes or the same polymer as p-doped in positive electrode and n-doped in negative electrode. In the asymmetric case the electrodes are made of different p-dopable polymers. Asymmetric or hybrid supercapacitors with one electrode being conductive polymer and the other electrode made of carbon have been made. Also composites consisting of conductive polymers and *e.g*. carbon nanotubes or metal oxides have been developed to improve capacitance, lifetime or conductivity. (Snook et al. 2011)

As mentioned earlier, pseudocapacitance can be obtained with oxide electrodes as well as conducting polymers. Of these, especially ruthenium dioxide RuO_2 and manganese dioxide MnO_2 have been studied. When charging and discharging a supercapacitor with oxide electrodes the oxidation states change. For RuO_2 specific capacitances of more than 600 F/g and for MnO_2 about 150 F/g have been reported. In the special cases of nanosized materials or thin film electrodes, values up to 1200 F/g for RuO_2 and 600 F/g for MnO_2 have been published. (González et al. 2016) Due to the price of ruthenium, RuO_2 electrodes are used only in small electronic devices. (Simon and Gogotsi 2008)

Materials such as activated carbon and conductive carbon are usually in powder form. Binder materials (Xiong et al. 2015) are thus needed in the electrodes to consolidate the materials. The binders also facilitate the adhesion of electrode material to current collector. The binders used in supercapacitor electrodes are usually polymers such as polytetrafluoroethylene (PTFE) or polyvinylidene difluoride (PVDF) and their concentration typically 5-10 wt%. (Ruiz et al. 2007) CMC (carboxymethyl cellulose) and SBR (styrene butadiene rubber) are also applied as binders (Varzi and Passerini 2015). Bio-based binders such as potato starch (Varzi and Passerini 2015) or casein from milk (Varzi et al. 2016) have also been developed. Obviously the mechanical integrity of the electrode requires a certain amount of binder but on the other hand excess binder decreases the energy density of the electrode since the binder does not contribute to forming the electrical double layer. It also masks the surface of activated carbon and thus reduces the capacitance.

When aqueous electrolytes are used, the hydrophobic nature of PVDF and PTFE make it difficult for the electrolyte to penetrate inside the electrode. Another disadvantage of these polymers is the fluorine, which makes the disposability and incineration more challenging. Dissolving fluorine containing polymers also often requires toxic and environmentally hazardous solvents. (Kouchachvili et al. 2014) However, PTFE and PVDF have also been used in supercapacitors having aqueous electrolytes. (Abbas et al.2014, Abbas et al. 2016) Combinations of polyvinylpyrrolidone/polyvinyl butyral (PVP/PVB) (Aslan et al. 2015) as well as chitosan hydrogel (Choudhury et al. 2012) and nanofibrillated cellulose (Blomquist et al. 2017) have been applied as electrode binder in supercapacitors with aqueous electrolyte.

2.3.2 Electrolyte

As previously mentioned, the choice of electrolyte affects many essential properties of supercapacitors, especially the voltage and temperature range as well as specific capacitance. Various electrolytes also result in different ESR values. Liquid electrolyte normally contains a solute dissolved in the solvent. Ionic liquids are here an exception since they consist only of ions and are solvent-free. It is also possible to use solid state or quasi solid state electrolytes. These types are shown in Table 2.4. Electrolyte can also be redox-active and participate in electrochemical reactions at the electrodes. (Zhong et al. 2016, Kötz and Carlen 2000) The redox-active electrolyte can be of water-based, organic, ionic liquid or gel polymer type.

TABLE 2.4. Classification and some examples of electrolyte types used in supercapacitors. (Zhong et al. 2015)

Liquid		**Solid or quasi-solid state**
Aqueous • Acid, H_2SO_4 • Alkaline, KOH • Neutral, KCl, Na_2SO_4	**Non-aqueous** • Organic, Tetraethylammonium tetrafluoroboride +acetonitrile • Ionic liquid, (EMIM)(BF_4) • Mixtures, (EMIM)(BF4)/acetonitrile	**Dry solid polymer** • PEO/LiCl **Gel polymer** • PVA/H_2SO_4+H_2O **Inorganic electrolyte** • Li_2S-P_2S_5

Although most commercial supercapacitor manufacturers use organic electrolytes, based on the number of publications in research and development aqueous electrolytes are more common. (Zhong et al. 2015) The reasons can include the low price, non-toxicity and non-flammability. Another advantage of water-based electrolytes is that organic solvents and ionic liquids need to be handled in special conditions, since moisture may lead to performance degradation and increased self-discharge. (Conway 1999) Obviously this leads to lower manufacturing costs for aqueous supercapacitors. (Brousse et al. 2013)

When water is used as the solvent, the solution can be acidic, alkaline or neutral depending on the solute. Typically aqueous electrolytes have relatively high conductivity which enhances the current output of the supercapacitor. Depending on the concentration, *e.g.* H_2SO_4 and KOH electrolytes can have ionic conductivities of over 500 mS cm^{-1} (Pandolfo et al. 2013) and NaCl solutions values of about 200 mS cm^{-1} (Wolf et al. 1985). The ionic conductivity of typical organic electrolytes is 10 – 60 mS cm^{-1}. (Pandolfo et al. 2013)

The advantages of neutral aqueous electrolytes compared with acidic or alkaline alternatives are larger potential windows, less corrosion and better safety. (Zhong et al. 2015) The drawbacks of neutral electrolytes are their lower specific capacitance and higher ESR. (Jimenez-Cordero et al. 2014) There exist several reports of using neutral aqueous electrolytes with cell voltage exceeding 1.2 V,(Abbas et al. 2016, Demarconnay et al. 2010, Fic et al. 2012, Abbas et al. 2015). The presence of hydrogen and hydroxide ions in acidic and alkaline electrolytes, causing lower overpotential for hydrogen and oxygen evolution, limits the electrochemical stable potential window to about 1.0 V. (Zhong et al. 2015) Due to the importance of the increase of energy density with higher voltage, safety and lower environmental impact, neutral electrolyte-based carbon supercapacitors have been identified as promising energy storage candidates. (Zhong et al. 2015)

The most commonly used organic electrolytes have acetonitrile (ACN) or propylene carbonate (PC) as solvent. The conductive salt can be *e.g.* tetraethylammonium tetrafluoroborate ($TEABF_4$). The accessibility of the electrolyte ions to the pores in electrode is obviously improved by decreasing the ion size. Since the large organic ions are not able to access as small pores as ions used with aqueous electrolytes, applying organic electrolytes often results in lower specific capacitance. (Zhong et al. 2015) Concerning the advantages of organic electrolyte, beside the higher voltage compared to supercapacitors with aqueous electrolyte, organic electrolytes facilitate the use of metallic materials such as aluminum as current collectors and encapsulation. (Zhong et al. 2016)

Ionic liquids are defined as salts composed only of ions with melting point below 100 ^{o}C. (Zhong et al. 2015) Ionic liquids have attractive properties for supercapacitor applications, especially high electrochemical stability giving a wide potential window, thermal stability and low vapour pressure. (Macfarlane et al. 2014) The voltage across the ionic liquid electrolyte can be 2 - 6 V, typically about 4.5 V. Since ionic liquids are solvent-free, they have no solvation shell, and thus they can offer a well identified ion size. (Wang et al. 2012) The main drawbacks of ionic liquid electrolytes are low ionic conductivity and high cost. Among ionic liquids (EMIM)(BF_4) has relatively high ionic conductivity of 14 $mScm^{-1}$, which is in the same range as lowest ionic conductivities for organic electrolytes. (Zhong et al. 2015) As already mentioned, the limited usability of ionic liquids at low temperatures also restricts their applicability.

2.3.3 Separator

The separator must be chemically and electrochemically stable, its porosity should be high to facilitate high ionic conductivity, it should be mechanically strong enough and it should tolerate the temperature range of the supercapacitor. (Zhong et al. 2015) Since the separator is a passive part of the supercapacitor, it should be thin, so as not to increase the volume of the component. Obviously the separator must prevent the short circuit between the electrodes and thus it has to prevent carbon particles of the opposite electrodes from touching each other. (Pandolfo et al. 2013) Paper separators consisting of cellulose fibres and having thickness 15 – 50 µm are typically used. Also glass-fiber as well as various polymers such as polyethylene (PE), polypropylene (PP), polyimide (PI) or polytetrafluoroethylene based separators have been reported. (Azaïs 2013)

2.3.4 Current collectors and encapsulation

To fully utilize the high power available from a supercapacitor cell it is essential to optimize all parts contributing to the ESR. The current collector is the electrical link between the electrode and supercapacitor external junction. Thus the resistance of current collectors and the contact resistance between the electrodes and current collectors should be made as low as possible (Azaïs 2013, Yan et al. 2014)

Besides good electrical conductivity, other critical current collector properties are electrochemical and chemical stability versus electrolyte, cost (purity and availability), density and processability. (Azaïs 2013) It is necessary to take into account the electrolyte since the current collector requirements for aqueous and organic electrolytes are different due to electrochemical stability issues typical for the electrolyte types.

With organic propylene carbonate and acetonitrile electrolytes, aluminum is the most popular current collector material. To improve the adhesion and decrease the contact resistance the surface of aluminum is typically roughened by electrochemical etching. To enhance the conductivity between the current collector and activated carbon electrode material, it is usual to make an interface layer of carbon black, graphite, carbon nanotubes or carbon nanofiber. (Azaïs 2013)

Aluminum current collectors are not compatible with water based electrodes since the acids, bases or aqueous salt solutions can cause corrosion. Possible metal alternatives include gold, platinum, titanium and stainless steel. (Yan et al. 2014) Graphite foil (Blomquist et al. 2017) or carbon paper (Li et al. 2011) current collectors have also been used with aqueous electrolyte to avoid corrosion. With carbon current collectors the low contact resistance between the carbon current collector and activated carbon electrode compared to the contact resistance between metal and activated carbon may decrease ESR. (Blomquist et al. 2017)

The encasing of supercapacitors can be made in various ways. The encapsulation protects the cell components mechanically, prevents the electrolyte from leaking out and keeps the impurities out. Commercial supercapacitor cells are typically rolled to form a cylindrical shape or stacked to coin-type structure. The rolls or stacks are then encapsulated inside cans or coin-cells made of metal. (Yu et al. 2013) Also pouch cell type encapsulation can be used in supercapacitor packaging. In this structure the cell is put between foils that are laminated together. The pouch cell design can result in low weight and the components can be made thin. (Yu et al. 2013) However, the pouch cells have relatively poor mechanical strength and polymer-based sealed encasing is not water and airtight for long-term application. (Azaïs 2013)

2.4 Printing and other solution processing methods

Solution processes such as various coating and printing methods can be scaled up to manufacture large number of devices or to coat large area substrates. This facilitates inexpensive manufacturing of electronic components and devices. The difference between printing and coating is that printing methods are able to create images that are shaped irregularly in two dimensions. (Ganz et al. 2016) There exist several printing methods such as screen, inkjet, gravure, flexo, and offset printing. (Suganuma 2014) All of these methods have characteristic properties such as line width, line thickness and speed.

The devices reported in this thesis were fabricated by rod coating or doctor blade method. A brief introduction to screen printing is however presented here due to the relevance of screen printing for scale up. (Keskinen et al. 2014)

2.4.1 Screen printing and rod coating

In commercial supercapacitors the thickness of activated carbon electrodes is typically of the order of 100 µm. (Azaïs 2013) Of the above-mentioned printing methods, screen printing is a feasible method for making layers of 5-100 µm thickness, while the other methods are typically used for thinner layers. (Suganuma 2014) Screen printing has been used to manufacture supercapacitor electrodes. (Lehtimäki et al. 2017, Wang et al. 2015) Pilot scale laboratory experiments of using screen printing in this application have also been reported. (Keskinen et al. 2014) In screen printing, printing is performed through a screen mesh with a pattern. The ink is first applied on the screen which is held slightly above the substrate. A squeegee is used for squeezing ink through the mesh onto the substrate. (Lawrence et al. 2004) The principle is shown in figure 2.9. The screen can be clamped at a frame like in the figure but also cylindrical meshes are used. In this case the method is called rotary screen printing and the screen is mounted onto a hollow cylinder. The squeegee is placed inside the cylinder and it squeezes the ink during rotation. (Ganz et al. 2016, Keskinen et al. 2014)

Other methods to apply solution layers having thickness of the order of 100 µm are blade coating or rod coating. Blade coating method is also known as doctor blade or knife coating. (Wengeler et al. 2013, Hösel 2013, Ganz et al. 2016) With blade coating layers of relatively uniform thickness can be applied on flexible or rigid surface. The thickness of the layer is defined by the distance of the blade from the substrate. Patterning is possible by using stencils through which the ink or paste is applied.

Rod coating is also called bar coating. In this method a wire-wound metering rod is used to apply liquid on substrate. (MacLeod 2007) Coating thickness is defined by the cross-sectional area of the grooves between the wire coils of the rod. Almost immediately after the rod has applied the liquid, surface tension makes the coating thickness uniform. In the same way as with doctor blade, stencil can be used to fabricate patterned coating.

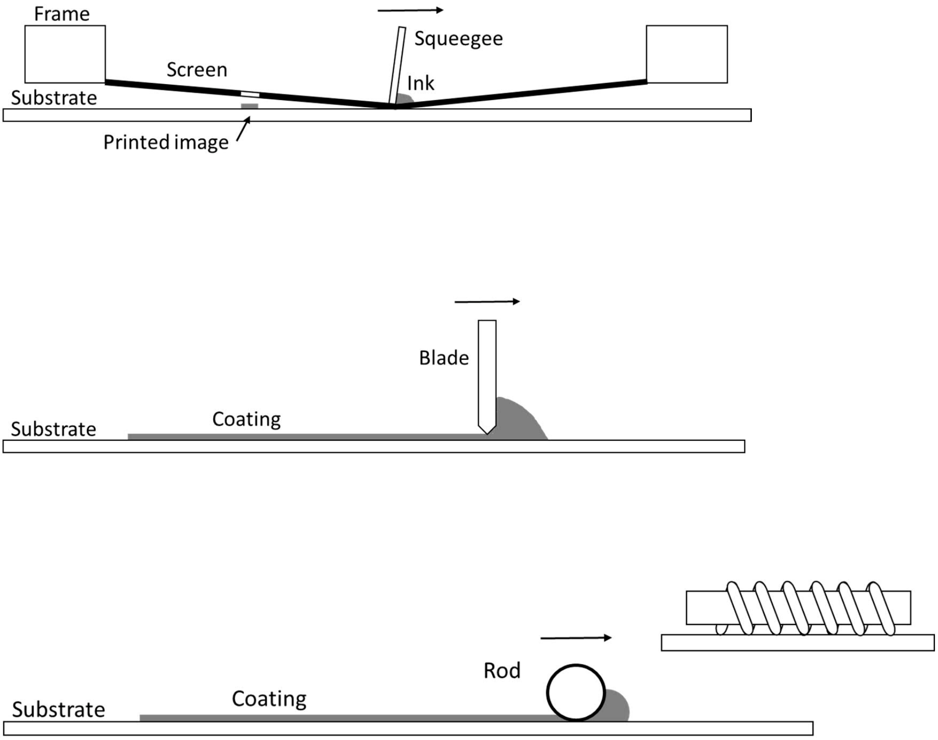

FIGURE 2.9. Principle of screen printing (up), blade coating (middle), and rod coating showing also the rod structure (low).

Blade and rod coaters are inexpensive and easy to operate. Laboratory scale single sheet coaters are available. The coaters are open systems, thus solvents are easily evaporated and the rheological behavior of the ink may change. The liquid flow at the blade or rod and near the substrate is very complex. (Ganz et al. 2016) It may be difficult to make a homogeneous film, since uneven thickness of the substrate easily results to an uneven film.

2.4.2 Curing and drying

Printing inks are applied as liquid or paste but must change to solid state before the next manufacturing step or using. Drying of the ink by evaporation after applying it removes the solvents. In some cases drying or curing processes include chemical changes such as polymerization and crosslinking. (Senich and Florin 1983) It is also often necessary to remove stabilizing agents located on the surfaces of the particles. Drying and curing are typically made in an oven or by using *e.g.* UV radiation, which are conventional postprinting processes in the printing industry. (Suganuma 2014) In many inks it is also necessary to improve the contact between particles. The contact can be enhanced by sintering at high temperature to utilize diffusion in the particles leading to necks between them. (Ganz et al. 2016)

3 Materials and methods

This chapter briefly describes the materials used, the methods to manufacture supercapacitors and characterization methods. The experimental details are described more in detail in the publications **I-IV**.

The choice of materials was largely made on the basis of requirements set for the devices. It was preferred to use non-toxic, recyclable and incinerable materials. Since the devices should be inexpensive to facilitate various applications, inexpensive materials were used.

The schematic structures of the two supercapacitor types are shown in Figure 3.1. The total thickness of the capacitor with packaging was typically about 0.6-0.8 mm, with the length and width being 40-80 mm and 40-50 mm, respectively. The key technical requirements for current collectors are that they should have low resistance and the electrolyte should not corrode them. Together with current collectors the substrates form the package of the component. Furthermore, the package should prevent the evaporation of electrolyte solution and provide the required mechanical strength.

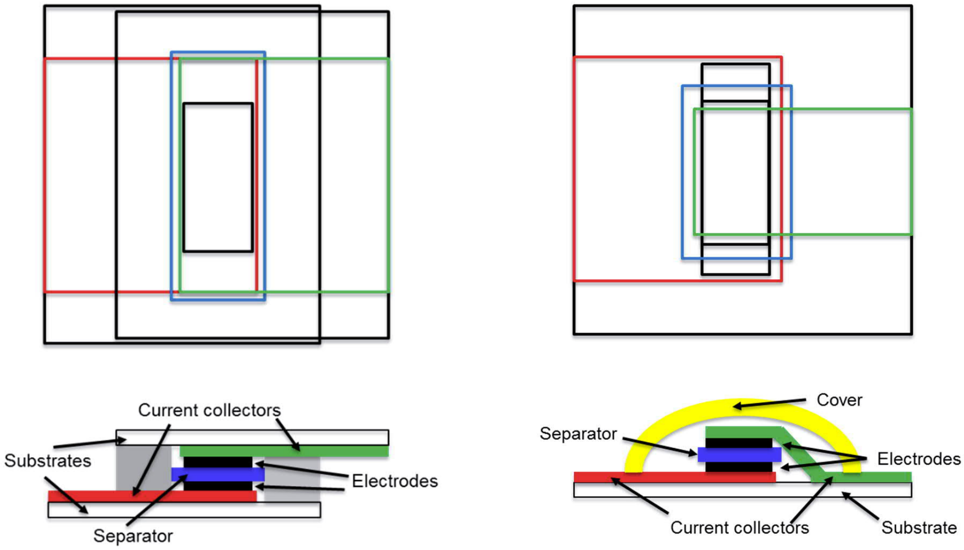

FIGURE 3.1. Schematic structures of supercapacitors: conventional face-to-face assembly (left) and monolithic structure (right).

3.1 Substrates and current collectors

The substrate materials used were paperboards and polymer films. These were coated or laminated with other materials to give required properties. Paperboard Stora Enso Cupforma Classic Barr 20 + 190 + 42EB56 was used in **I** and **III**. It is coated with polymer on both sides and on one side the polymer layer is designed to improve barrier properties against oxygen and water penetration. Polyethylene terephthalate (PET) foil was used as such only in **IV** and laminated with aluminum foil in **II**, **III** ja **IV**. The aluminum acted in some cases both as current collector and barrier layer to prevent oxygen and moisture penetration and in some cases only as barrier layer. In **III** also PET foil coated with copper was used to enhance the electrical conductivity of the current collectors.

All current collector structures included a layer of graphite ink Acheson PF407C. In several cases it was used as such (**III**, **IV**) but also on top of either aluminum foil (**II**, **III**) or silver ink (**I**, **III**) to prevent metal corrosion caused by aqueous electrolyte. The graphite ink was applied by the doctor blade method. The ink is made especially for screen printing, and its applicability in screen printed supercapacitor current collectors has been proven. (Keskinen et al. 2014) The graphite ink curing temperature was chosen to be 95 ^{o}C in all cases to avoid damage to polymer coatings or films.

3.2 Electrodes

In all supercapacitors described in **I**-**IV** the carbon based electrodes were made of activated carbon in powder form. Norit DLC Super 30 was used in **I**, **II** and **III** and Kuraray YP-80F in **III** and **IV**. The specific surface areas of these are about 1500 m^2/g (Balducci and Schütter 2015) and 1900-2200 m^2/g (Kuraray 2017), respectively. The reason for changing the type was that Norit discontinued the production of supercapacitor grade activated carbon. Chitosan was used as binder in the electrodes. The chitosan grades used were Primex ChitoClear fg90 (**I**, **II**, **III**) and Sigma-Aldrich 50494 (**III**, **IV**). Also in this case the reason for change was the unavailability of the Primex grade. The activated carbon inks were synthesized by first dissolving the chitosan in mild acetic acid solution. Then activated carbon was mixed to the solution. The mass ratio of activated carbon to chitosan was about 18:1. The activated carbon inks were applied by bar coater (**I**, **II**, **III**) or doctor blade (**III**, **IV**). In the same way as in the case with current collectors, these inks have also been applied by screen printing. (Keskinen et al. 2014)

In **II** polypyrrole (Ppy) was used as electrode material. The Ppy sheets were received from Uppsala University and printed Ppy electrodes were made at VTT in Espoo and thus the synthesis and processing of the sheets and inks are outside of the scope of this thesis.

3.3 Separators

Paper separators were used in most supercapacitors. The NKK TF40-50 cellulose separator used in **I**, **II** and **III** was replaced in later experiments (**III** and **IV**) with Dreamweaver Silver AR40. The reason was that when moistened with aqueous electrolyte the dimensions of Dreamweaver change less making the assembling easier. In one experiment in **I** porous Whatman Nuclepore polycarbonate separator was used. In **IV** the chitosan separator used was made of Sigma-Aldrich 50494. One of the chitosan separators included also talc (Finntalc M15E).

3.4 Electrolytes

All the supercapacitors manufactured had aqueous electrolyte made of de-ionized water and salt. In **I**, **III** and **IV** the salt used was sodium chloride (NaCl). The NaCl to water mass ratio of 1:5 corresponding about 3.2 M was used in **I**, **III** and **IV**. In **I** mass ratios of 1:20 and 1:4 were also tested. In **II** sodium nitrate ($NaNO_3$) buffered to pH 7 either in liquid (5 M) or gel (0.67 M) form was used.

3.5 Layout and assembling process

The printed supercapacitor electrodes were assembled to components so that activated carbon layers were face-to-face. A frame made of polyethylene (PE) was placed around the active layer and the separator to prevent short circuit between the two current collectors in cases where the layout made this necessary. For adhesion of the top and bottom electrodes, a hot melt foil (Collano TEX-B 384) or Paramelt Aquaseal X2277 polyolefin dispersion were used. The change in material was necessary due to the end of availability of the hot melt foil and also to facilitate the liquid processing of the material. The heat sealing was performed using a device which pressed the area to be sealed simultaneously giving a heat pulse.

The manufacturing process of the layer-by-layer fabricated monolithic supercapacitors started by applying the lower graphite ink to act as current collector. On top of that activated carbon layer was applied. Dreamweaver cellulose paper or chitosan to act as separator was added. On top of the separator the upper electrode and the upper current collector were applied. When these layers were ready, the electrolyte was added. The alternatives for encapsulation were the same materials used as substrate or epoxy (Loctite Power Epoxy Universal). The foils used as top encapsulation were heat-sealed using the polyolefin dispersion.

3.6 Characterization of electrical properties

The electrical properties of the supercapacitors such as capacitance, equivalent series resistance (ESR), and leakage current were determined using an industrial standard. (IEC 2006) An Arbin SCTS instrument was used in **I**, **II** and **III** and a Maccor 4300 in **III** and **IV**. The basic measurement cycle is shown in figure 3.2. The component was first charged and discharged with constant current up to 1.2 V three times, and then the voltage was kept for 30 minutes at 1.2 V and discharged with a constant current. The capacitance was defined during the constant current discharge step between 0.96 V and 0.48 V voltage. The ESR was obtained from the voltage drop in the beginning of this discharge step. This abrupt change is called IR drop and ESR is calculated by dividing the voltage drop with the current used. The efficiency was defined as the ratio of the discharged and charged energy in the voltage range of 0 – 1.2 V or 0.2 – 1.2 V. The leakage current of the supercapacitors was determined with a float current experiment: the capacitor was charged to 1.2 V and the current recorded after holding that voltage for 1 hour. For some capacitors, self-discharge was also measured by charging the capacitors for 1 h or 24 h with a constant voltage of 1.2 V, then disconnecting the capacitor from any outside circuits and manually checking the voltage level with a multimeter (input impedance 10 MΩ) for up to about 30 days. In **II** the maximum voltage was either 0.6 or 0.8 V instead of 1.2 V.

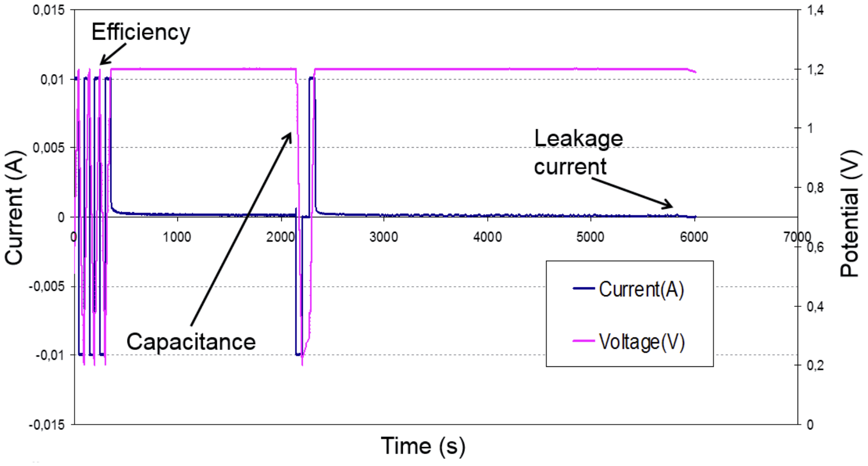

FIGURE 3.2. Measurement procedure showing the voltage profile and the resulting current.

The two-electrode cyclic voltammetry (CV) characterization was performed in **II** with the Arbin SCTS system using either 0.1-0.6 V or 0.1-0.8 V range and in **IV** with the Maccor 4300 system in the voltage range 0-1.2 V.

4 Results and discussion

The aim of the work was to develop novel concepts for low-cost thin supercapacitors using environmentally benign materials. Thus the main emphasis was in finding feasible material alternatives to be applied in electrodes, current collectors and encapsulation as well as electrolytes. Further, the structure and layout of the supercapacitors needed to be designed to exploit the possibilities offered by these materials.

4.1 Paperboard and polymer substrates

4.1.1 Supercapacitor fabrication and functionality

Flexible substrates were used both to facilitate roll-to-roll (R2R) manufacturing and to allow applications on curved surfaces. Flexibility is beneficial *e.g.* in wearable applications. In **I-IV** all the experiments were made on sheet materials, but flexibility during the manufacturing process was demonstrated in R2R printing experiments done at VTT Oulu using the same current collector and electrode inks which were applied in the sheet process. (Keskinen et al. 2014)

An additional advantage provided by paperboard and polymer (PET) substrates is their relatively easy recycling. They are also incinerable with normal household waste. Both paperboard and polymer substrates are inexpensive and do not limit the feasibility of using these components also in applications where expenses are critical. The choice between polymer and paperboard obviously depends on the requirements set to the component. *E.g*. in cases when there is an existing package made of paperboard or PET to which the supercapacitor is to be integrated it may be cost-effective to use the same material also as supercapacitor substrate. On the other hand PET is a more durable alternative *e.g.* in humid or wet environments.

Figure 4.1 shows an example of supercapacitor electrodes made on polymer coated paperboard. The silver ink (grey area) is first applied on the substrate and then graphite ink on top of it. Since the silver ink has relatively high conductivity it decreases the ESR of the supercapacitor. The graphite ink protects the silver from the corrosion caused by the aqueous electrolyte. It may also decrease the contact resistance between the activated carbon electrode and silver current collector. Another advantage of the graphite ink is that it improves the barrier properties by decreasing the evaporation of water from the electrolyte as well as oxygen penetration from air to the electrolyte.

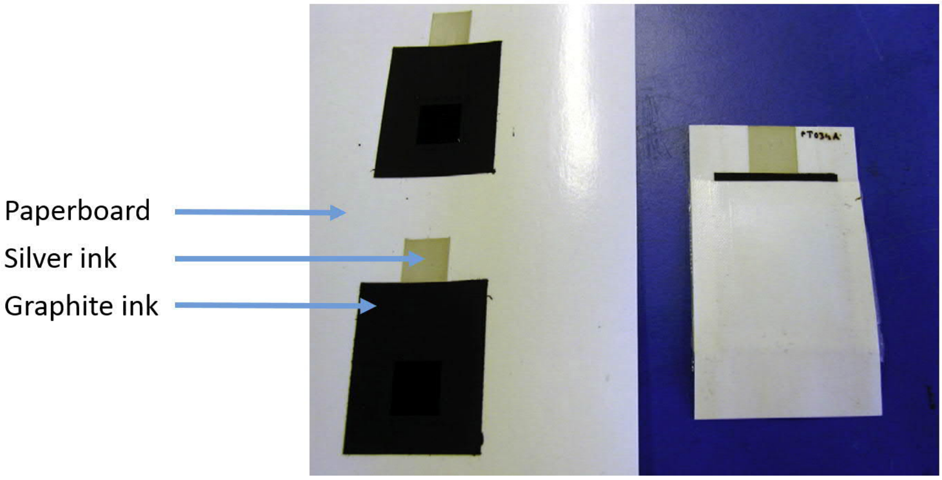

FIGURE 4.1. Electrodes with current collectors made of silver and graphite ink on paperboard substrate (left) and a face-to-face assembled supercapacitor using these electrodes. Adapted from **I**.

Besides silver ink, metal foil can also be used as metallic current collector. If aluminum-polymer laminate is used as substrate, the aluminum layer can act as current collector. Simultaneously aluminum acts also as a barrier to water and oxygen. Examples of supercapacitors having Al/PET substrate with electrode structure on aluminum side are shown in Figure 4.2.

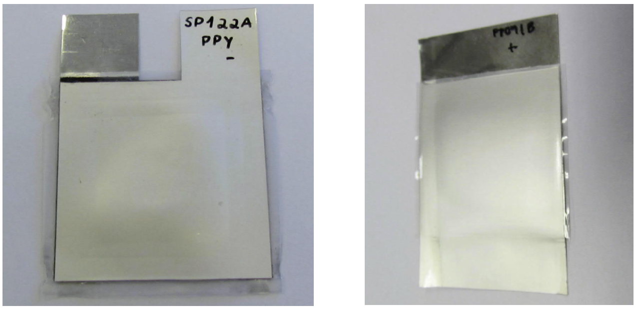

FIGURE 4.2. Supercapacitors with electrodes made on aluminum/PET laminate. In both cases the aluminum layer of the laminate acts as current collector. Adapted from **II** and **III**.

Due to occasional corrosion issues with the combination of aluminum current collectors and aqueous electrolyte, supercapacitor electrodes were fabricated without metallic current collectors. In practice, the Acheson PF407C graphite ink layer between the electrode and aluminum layer could not prevent the penetration on aqueous electrolyte to the surface of aluminum. Thus when low ESR was not required, graphite ink alone acted as current collector. This was the case in several face-to-face assemble supercapacitors (**III**) and in all monolithic devices (**IV**). A supercapacitor with Al/PET laminate as substrate utilizing aluminum layer only as barrier layer and a monolithic supercapacitor with PET alone as substrate are shown in Figure 4.3.

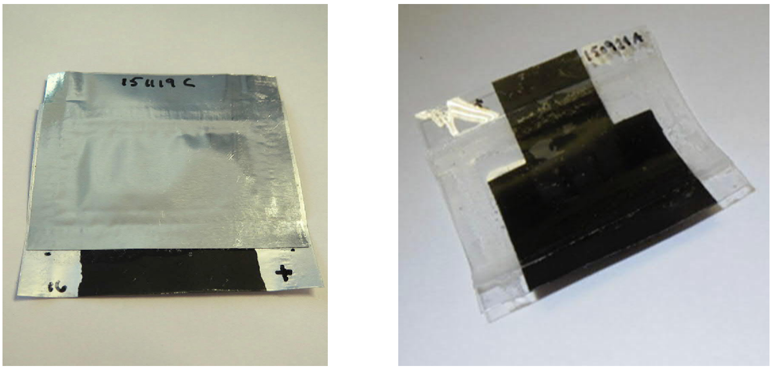

a b

FIGURE 4.3. A supercapacitor with electrode structure on the PET side of an Al/PET substrate (a) and a monolithic supercapacitor on PET substrate (b). Adapted from **III** and **IV**.

4.1.2 Lifetime

Obviously it is essential to minimize the evaporation of water from the aqueous electrolyte through the encapsulation. When water evaporates, the salt content increases and when the maximum solubility of the salt is reached, solid salt crystallizes inside the electrolyte. The electrical conductivity of crystalline salt such as NaCl is very poor when the ions are immobile. Simultaneously, the solidified salt prevents the electrical double layer formation of the surface of activated carbon electrolyte. Thus the electrical properties deteriorate.

The mass of the electrolyte in supercapacitors having 2 cm^2 geometrical electrode area was about 200 mg. When Cupforma Barr or graphite ink coated PET were used as substrate, the mass loss of a supercapacitor was of the order of 5 mg/week (**III**). This evaporation rate limits the lifetime of the supercapacitor to a few months.

Figure 4.4 shows the electrolyte mass as a function of time for various supercapacitors made on paperboard substrate. The mass decreases due to the evaporation of electrolyte through the substrates. The energy efficiencies (η, unit %) of the supercapacitors are shown beside the data points. The increase of mass in some cases during the first days is presumably due to the fact that the paperboard dried during the curing of silver and graphite inks and absorbed some moisture from air during the next few days. The points with marker type 1, 2 and 5 belong to supercapacitors made on the PE side of the Stora Enso paperboard. Of these 1 and 2 have narrow graphite layers instead of wide graphite layers on top of the silver current collectors. Thus the electrolyte has been in contact with the PE coating. These supercapacitors show the fastest electrolyte evaporation rate. In the supercapacitor marked with 5 the graphite layer was wider, covering the whole PE coating from the electrolyte side. It can be seen that the wide graphite ink layer clearly decreased the electrolyte evaporation rate. In samples 3 and 4 the electrode was made on the barrier layer side of the paperboard. Of these sample 3 had the narrower graphite layer and in sample 4 the graphite layer covered the whole area in contact with electrolyte. The electrolyte mass loss of sample 4 was about 0.05 g in 90 days whereas similar mass loss took place in samples 1 and 2 in about 10 days. The effect of the graphite ink layer on the barrier properties is remarkable. Especially with the poor barriers such as PE (sample 3 compared with samples 1 and 2) the improvement is clear, but also with the polymer barrier foil on the paperboard (samples 4 and 5) the additional barrier provided by the graphite ink decreased the mass loss from about 0.07 g to the above mentioned 0.05 g during the measurement period.

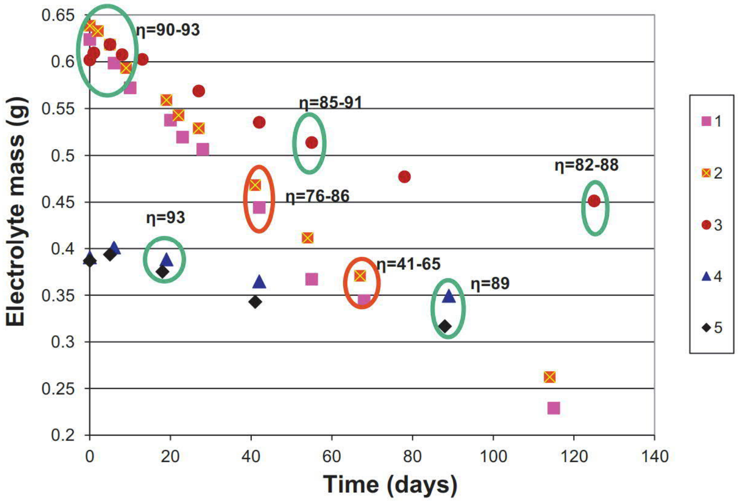

FIGURE 4.4. Electrolyte mass as a function of time for supercapacitors having various substrate and current collector alternatives. Energy efficiency values are shown beside some of the points. Sample codes 1-5 are explained in the text. Adapted from **I**.

When Al/PET laminate was used as substrate, the evaporation rate was measured to be 0.01-0.3 mg/week. The variation in the rate is largely due to differences in the sealing materials and processes. Thus with aluminum barrier the evaporation rate of the electrolyte is very low and the salt concentration inside the supercapacitor remains at the correct level for several years.

Cycle lifetime up to 40000 cycles was measured for a supercapacitor made on Al/PET laminate. In this case aluminum served as current collector (**III**). Figure 4.5 shows the change of capacitance, energy efficiency and leakage current as a function of the number of cycles. The original capacitance was 0.45 F and decreased to 0.41 F during the test. Also decrease of energy efficiency from 96 % to 90 % was detected. As typical with most of the supercapacitors made in **I-IV**, leakage current reduction during cycle tests of constant voltage floating was observed. This can be partly associated with activated carbon pores filling with ions. When charged for the first time, the ions do not reach the pore surfaces completely but when the charging is continued, the filling is more even. In the case the ions do not cover the whole surface, their redistribution is observed as a voltage decrease. To maintain the voltage level current input is required.

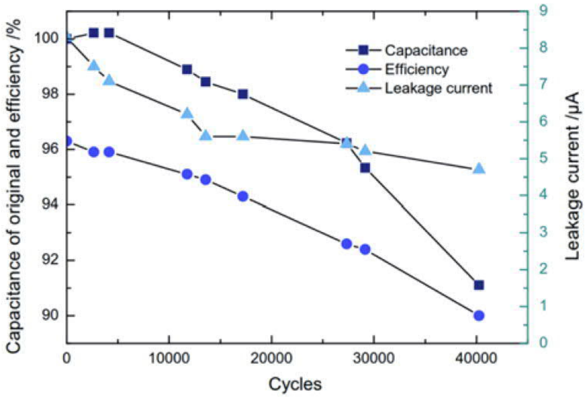

Figure 4.5. Cycle life test during which capacitance, energy efficiency and leakage current have been determined. Adapted from **III**.

4.1.3 Leakage current and self-discharge

Self-discharge can be defined as the rate of voltage change, i.e. voltage change per time unit, when the supercapacitor is in open-circuit state. In case two supercapacitors of different capacitance have the same self-discharge rate, their leakage current values have the same ratio as their capacitance values.

Table 4.1. Supercapacitor types reported concerning leakage current and self-discharge (**III**)

Type	**Substrate**	**Current collector**	**Activated carbon**	**Sealing**	**Separator**	**Al barrier**
A	Paperboard	Ag-ink + graphite ink	Norit	Collano	NKK	No
B	Paperboard	Al-foil + graphite ink	Norit	Collano	NKK	Yes
C	Al25/PET23	Al from substrate+graphite ink	Norit	Collano	NKK	No
D	Al7/PET100	Al from substrate+graphite ink	Norit	Collano	NKK	Yes
E	Cu/PET125	100 nm evaporated Cu + graphite ink	Kuraray	Paramelt	Dreamweaver	No
F	PET50/Al9, electrode on PET side	Graphite ink	Kuraray	Paramelt	Dreamweaver	Yes

Figure 4.6 shows the leakage current for various supercapacitor structures. The structure of each capacitor type present in the figure can be found in Table 4.1. As expected, the increase in capacitance generally results in higher leakage current if the structure remains the same. The components having blue markers (A, C, E) in the graph have no continuous metallic layer between the electrolyte and outside air. Thus it can be expected that they may have higher oxygen content in the electrolyte due to poorer barrier against oxygen penetration through the substrate. On average, these three supercapacitor types have higher leakage current relative to their capacitance than the other three types (B, D, F) having metal a layer acting as an oxygen barrier.

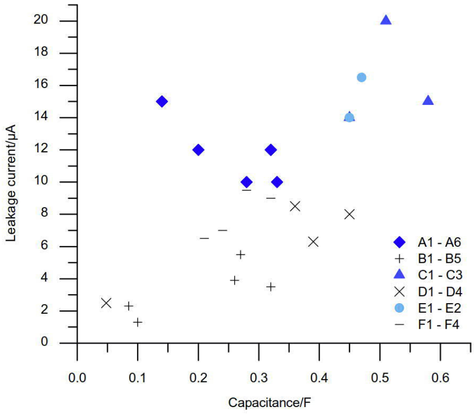

FIGURE 4.6. Leakage current of various supercapacitors as a function of capacitance. The sample codes refer to Table 4.1. Adapted from **III**.

The self-discharge rate of a supercapacitor made on paperboard is shown in Figure 4.7 a. In the experiment the supercapacitor was kept at 1.2 V for 1 hour before disconnecting it and after that its voltage was recorded as a function of time. The leakage current of similar devices was of the order of 10-20 µA after 1 hour floating at 1.2 V (**I**). In Figure 4.6 this structure is represented by the group of supercapacitors of type A.

Figure 4.7 b shows the self-discharge rate for two different types of devices. Type E has 125 µm PET substrate with copper frame and the substrate of type F is Al/PET foil with 9 µm thick aluminum laminated on 50 µm thick PET. Thus the barrier properties of type F against oxygen penetration through the substrate to electrolyte and against water evaporation from the electrolyte are better than those of type E supercapacitors. Increased oxygen content has been associated with higher leakage current (Hahn et al. 2000) and this would explain the difference in self-discharge behavior between the types E and F. Besides the difference in self-discharge rate between devices having various substrates, the floating time at constant voltage before starting the self-discharge test is of importance. The reason was already discussed above when leakage current was dealt with: the redistribution of ions in activated carbon pores is seen as self-discharge (**III**).

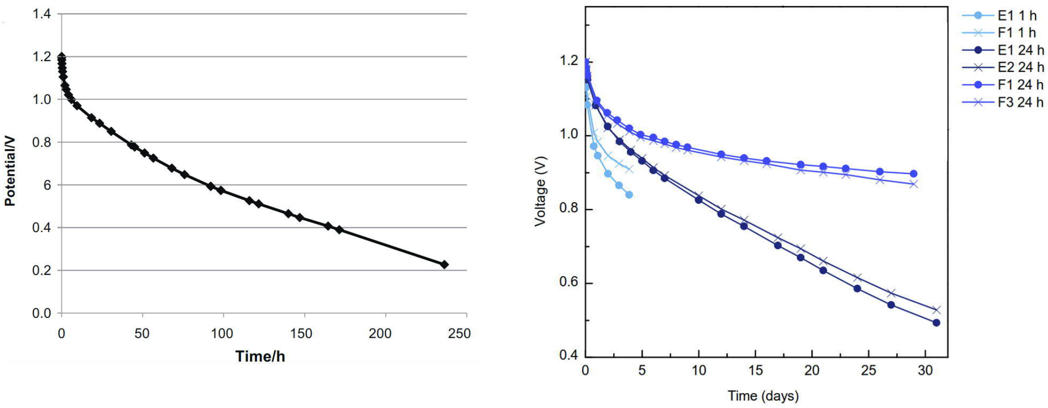

a

b

FIGURE 4.7. Self-discharge rate for a supercapacitor on paperboard (a) and for supercapacitors on PET or Al/PET substrates. Adapted from **I** and **III**.

The instantaneous leakage current during the self-discharge experiments was defined from the voltage change between consecutive voltage measurement points by taking the capacitance and time interval between the points into account. Figure 4.8 shows the voltage (dashed lines) and leakage current (continuous lines) as a function of time. The sample types are E and F as described above. The leakage current values start from µA range but when the voltage decreases due to self-discharge, the instantaneous leakage current decreases. Especially with the sample F having aluminum as a barrier layer, after floating for 24 hours the leakage current reaches very low values. After two days the leakage current is only about 100 nA and the voltage is about 1.05 V. In 20 days the voltage has reached 0.92 V and the instantaneous leakage current is 10 nA. After 30 days the voltage is 0.89 V. Thus according to the equation 2.6, 55 % of the original energy at 1.2 V is still remaining in the supercapacitor.

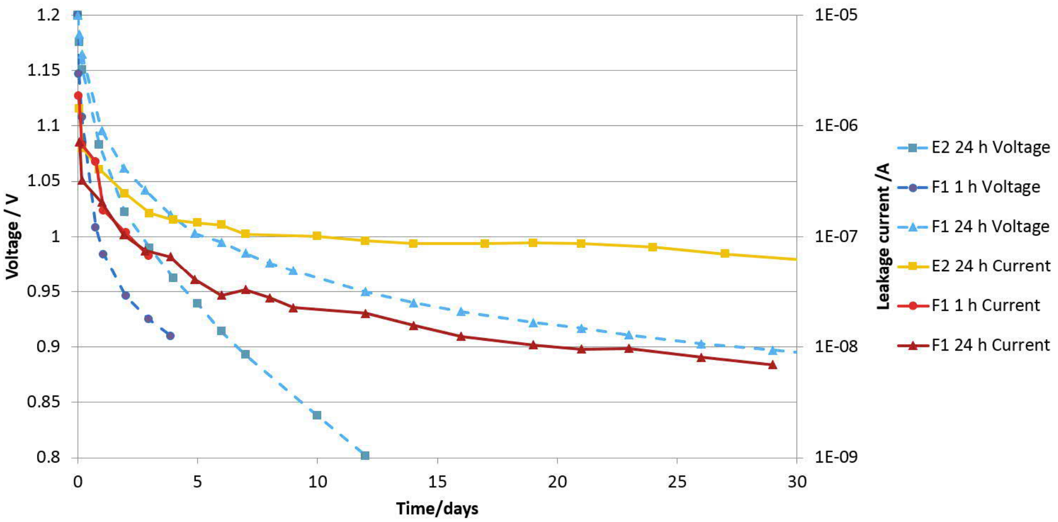

FIGURE 4.8. Voltage and respective instantaneous leakage current during supercapacitor self-discharge.

Based on the analysis in **III**, the self-discharge is most probably due to Faradaic reactions of impurities such as oxygen. The impurities on the surface of activated carbon powder and in chitosan used as binder may also increase the self-discharge rate. Thus to further limit the self-discharge, purer materials and careful removal of oxygen while maintaining good barrier properties could be beneficial.

4.2 Current collector structure

4.2.1 Requirements for current collectors

The current collector layers have several requirements. Obviously their task to conduct electricity demands low resistance. They must also be chemically compatible with their environment and, in case of low-cost components allow inexpensive manufacturing techniques and naturally not contain expensive materials. From an environmental point of view, toxic materials should not be used and recyclability or the possibility to incinerate the material would be beneficial.

The lower the resistance of current collector, the lower are also the losses due to charge and discharge current. The current collectors connect the electrodes to the outside of the encapsulation, and thus the current collectors must not be open-porous, since otherwise the electrolyte would leak out through them. Also oxygen from air should not penetrate through the current collectors to the electrolyte. From the sealing point of view not only the bulk properties of current collectors are important, but also the adhesion between the current collector and substrate or sealing material must be good enough to facilitate hermetic packaging.

To keep the manufacturing process simple, the current collectors were either made of inks using solution processes or multilayer foils including metal (aluminum or copper) and polymer layers. Some tests were also made with separate aluminum foils which were glued on paperboard substrate. The inks included either silver or graphite as conductive component. Due to the corrosion of metal when in contact with salt containing water, the metal layers were coated with graphite ink. In applications where especially low ESR is not required, graphite ink alone was used as current collector to avoid the issues with corrosion.

The dimensions of current collector are also of great importance. To reach reasonably low ESR, in the case of bulk metallic current collector the thickness and width (i.e. cross-sectional area) may be relatively small and the length need not necessarily be minimized. If silver or especially graphite ink acts as a current collector, it may be important to make it thick and wide enough as well as keep the current path short.

4.2.2 ESR

As discussed above, the ESR of a supercapacitor consists of the Ohmic resistance the components of which are current collectors and activated carbon layer and the ionic resistance in the electrolyte. Beside these there is also contact resistance between the layers.

The orders of magnitude of the resistance of various current collector alternatives used in **I**-**IV** are shown in Table 4.2. The silver and graphite ink resistances are for geometry that could be used in the supercapacitors of the type reported in this study. The aluminum foil thickness is typically of the order of 10 µm, the actual thicknesses used in **I**-**IV** being 7-23 µm. The resistance for copper is calculated for the case used in **III**, where 100 nm thick copper layer had been deposited on PET.

Table 4.2. Resistivity and resistance values for various current collector alternatives.

	Resistivity	**Square resistance for 25 µm thick layer**	**Slab resistance, length 40 mm, width 20 mm**
Silver ink Acheson Electrodag PF 410		<0.025 Ω/sq (Electrodag PF 410 2018)	<0.05 Ω Thickness 25 µm
Graphite ink Acheson Electrodag PF 407C		<20 Ω/sq (Electrodag PF 407C 2018)	< 40 Ω Thickness 25 µm
Aluminum	2.65 x 10^{-8} Ω m (Engineering Toolbox 2018)		0.0053 Ω Thickness 10 µm
Copper	1.72 x 10^{-8} Ω m (Engineering Toolbox 2018)		0.34 Ω Thickness 100 nm

When graphite ink alone is used as current collector, the ESR values are obviously also affected by different graphite ink layer thicknesses. The manufacturer has reported the square resistance for each graphite ink batches and they are about 11 - 14 Ω/sq for 25 µm thick layers. Since the thickness of the cured current collector ink is typically 20 - 30 µm and the shape of the current collector is designed to be as wide and as short as possible, the total resistance of two current collectors can be estimated to be of the order of 10 - 30 Ω.

The resistivity of the cured activated carbon electrode ink is 0.70 Ωm (**IV**). Using this value together with the dimensions of the electrodes (typical area 2 cm^2 and thickness 50-100 µm), the resistance of each electrode is 0.17 - 0.35 Ω. The ionic conductivity of the aqueous electrolyte used (1:5 NaCl:water) is 0.184 S/cm (Wolf et al. 1985) from which the ionic resistance is 0.0543 Ωm. If the average thickness of the electrolyte is 0.1 mm and area 2 cm^2, the ionic resistance originating from the electrolyte would be 0.027 Ω. In practice the separator and the porosity of electrodes increase this value.

When the above resistance values of supercapacitor are compared, it is evident that when graphite ink current collectors are used, they cause the majority of the ESR. On the basis of the figures in Table 4.2 and the calculated resistance values, with metallic or metal ink current collectors most of the ESR originates from the electrodes and electrolyte and possibly also from the contact resistances between the materials.

The ESRs of supercapacitors with activated carbon electrodes and conventional face-to-face assembly are shown in **III**. For devices with 2 cm^2 geometrical electrode area having metallic current collectors using either silver ink or aluminum foil, the ESR is of the order of 1 Ω. Obviously the ESR becomes higher for smaller electrode area when the thickness of the electrodes and electrolyte layer are kept constant.

Figure 4.9. shows charge and discharge curves with constant current for supercapacitor types A - F (described in Table 4.1). Their ESR can be estimated from the IR drop when the direction of the current is changed. Although the IR drop is present in all curves, it is clearer in case of supercapacitors having higher ESR (E and F) and when the higher current of 10 mA has been used. The IR drop shown in this case is double compared to the IR drop when the supercapacitor has been kept at constant voltage (Figure 3.2) before discharging. This is due to fact that when charged with constant current just before the discharge step there is voltage difference across the ESR both during charging and discharging.

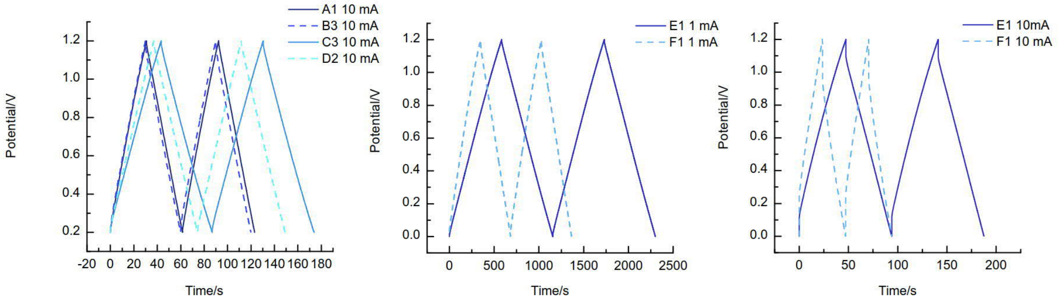

FIGURE 4.9. Constant current charge/discharge curves for various types of supercapacitors. Adapted from **III**.

4.2.3 Corrosion

The supercapacitors made on paperboard had silver ink current collectors covered with graphite ink (**I**, **III**). In **III** a structure where a separate aluminium foil covered with graphite ink was reported. Since paperboard is non-transparent, it is not possible to observe if the aluminium foil or the silver ink have any visible damages. However in the case that the electrolyte evaporation rate through the encapsulation is relatively high, resulting in electrolyte drying in a few months, the corrosion caused by the aqueous electrolyte may not become a problem during the lifetime of the supercapacitor.

With Al/PET laminate the corrosion becomes clearly visible. Since the aluminum in these laminates is quite thin, *e.g*. 7 or 9 µm, the corrosion points become quite quickly visible through the PET layer. Figure 4.10 shows an example of a supercapacitor with the holes corroded through aluminum showing the graphite layer. The consequences are that the electrochemical reactions considerably deteriorate the electrical properties of the supercapacitor and the barrier properties of aluminium are lost. When the corrosion takes place near the edges, they can cause electrolyte leakage from the supercapacitor.

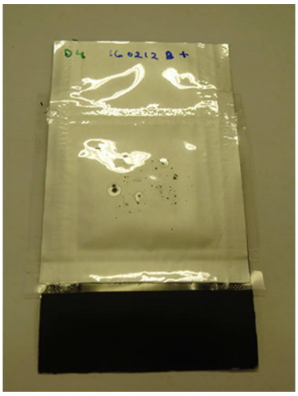

FIGURE 4.10. An example of corrosion of aluminum current collector due to poor protection by graphite layer.

Figure 4.11 shows a supercapacitor on a 125 µm thick PET substrate on which there is 100 nm of evaporated copper to improve electrical conductivity and decrease the ESR value. The copper layer is etched away from the area that covers the electrolyte. The motivation for the etching was to avoid copper corrosion due to electrolyte penetration through graphite ink layer. Compared to graphite ink alone, the copper frame provided better current collector conductivity resulting to lower ESR. Compared to the device with graphite ink only as current collector the ESR was about 50 % lower. The drawback is that in this structure there is no metallic barrier against oxygen or water vapor penetration. Obviously this could be overcome by having *e.g.* an aluminum layer on the PET foil on the opposite side of the copper coating.

Figure 4.11. Copper frame to avoid metal corrosion and improve electrical conductivity. Adapted from **III**.

4.3 Electrode materials

In most of the supercapacitors developed in this work electrodes were made of ink containing activated carbon powder and chitosan. The activated carbon grades used were developed by their manufacturers to be used in supercapacitors. The binder of choice was chitosan since it can be dissolved in mildly acidic water without organic solvents and after drying it has mechanically strong structure.

The motivations to use alternative electrode materials are increasing specific energy or power. To investigate the possibility to increase specific capacitance, in this work polypyrrole was used as supercapacitor electrode with *Cladophora* cellulose as binder.

4.3.1 Activated carbon

The morphology and particle size of an activated carbon electrode can be seen in the scanning electron micrograph (SEM) shown in Figure 4.12. The figure shows Kuraray activated carbon with chitosan as a binder. As can be seen, the particle size is of the order of 1-10 µm and the shape is irregular. Although the electrode has about 5 mass% of chitosan of the total dry mass, it is not clearly visible in the micrograph.

The concentration of chitosan was not optimized. A rough experiment showed that there was no clear visible or mechanical difference between 5 and 10 mass%. Thus the lower concentration was chosen to have higher electrically active area in the electrode relative to its total mass. Besides chitosan some experiments were done with polyvinyl acetate (PVAc) and polyvinyl butyral (PVB) as a binder material together with the Kuraray activated carbon. These trials resulted in mechanically strong structure but both PVAc and PVB bound electrodes exhibited about 80 % lower specific capacitance and even with the naked eye it was possible to observe poorer wetting of electrodes with these binders compared to the situation with chitosan.

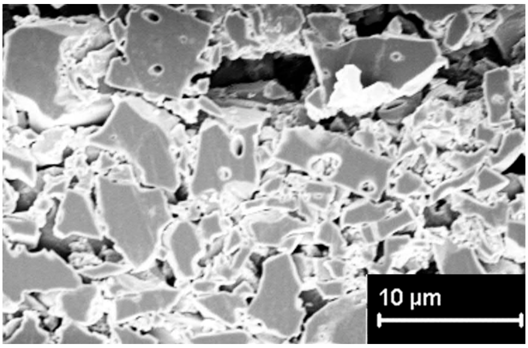

FIGURE 4.12. Cross-section of activated carbon electrode, broad-ion-beam processed surface.

4.3.2 Conductive polymer electrode

In this study both symmetric and asymmetric supercapacitors with polypyrrole electrodes were fabricated (**II**). In the asymmetric case the other electrode was made of activated carbon. The manufacturing method for activated carbon electrode was similar to the method used in **I**, **III** and **IV**.

Based on the measurements(**II**), the specific capacitance for the Ppy electrode was defined to be 211 F/g for the printed electrode and 172 F/g for the sheet type electrode. These are clearly below the theoretical (620 F/g) and reported (530 F/g) for Ppy. (Snook et al. 2011) However, the values are considerably higher than the specific capacitance of the Norit activated carbon (90 F/g). Thus using a symmetric Ppy supercapacitor structure would potentially give the highest specific capacitance for the device.

A device with symmetric PPy electrodes was charged and discharged with constant voltage sweep rate. The results of the experiment are shown in Figure 4.13 (a). The charge/discharge cycling was interrupted after various number of cycles and CV measurement was performed. The first 330 cycles were done between 0.1 and 0.6 V and after that between 0.1 and 0.8 V. The CV curves show clear deterioration of properties. Thus the symmetric device could find little use in practical applications. Significantly longer cycle life was obtained for an asymmetric structure with activated carbon positive electrode, Figure 4.13 (b). After over 14000 charge/discharge cycles the device still showed a relatively rectangular CV curve indicating only little degradation compared with the symmetric supercapacitor.

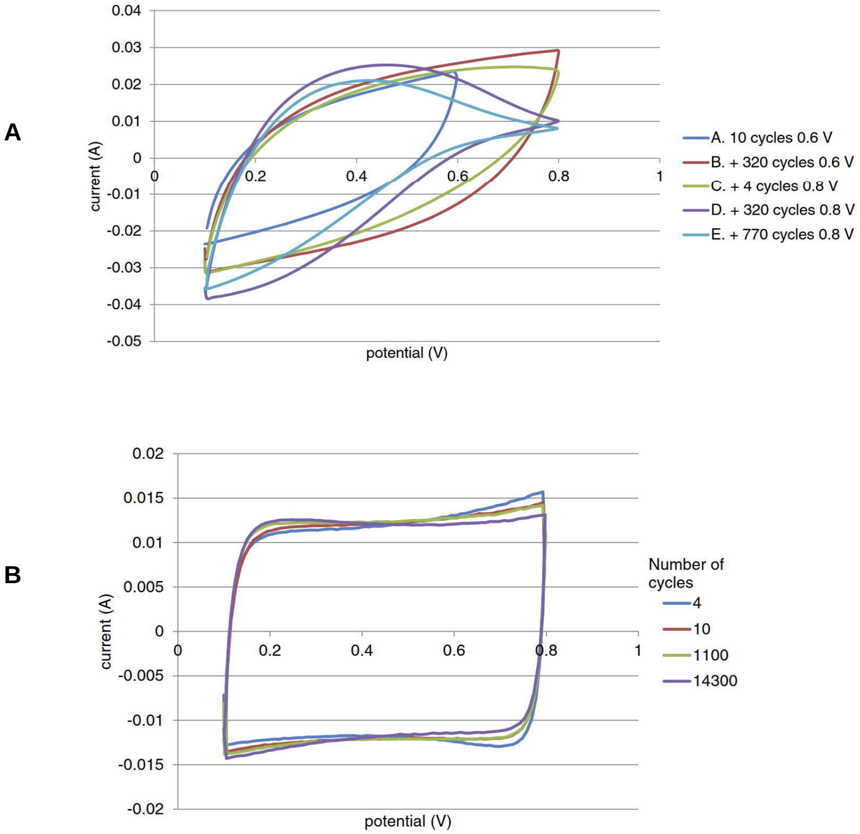

FIGURE 4.13. CV for supercapacitor with symmetric Ppy electrodes (a) and with positive electrode made of activated carbon and negative of Ppy (b). Adapted from **II**.

As can be estimated also from the CV curves belonging to the asymmetric device, its capacitance decreased during the cycling. When new, the capacitance defined from the data obtained from constant current cycles was about 1.29 F and gradually decreased to about 1.23 F after 14300 cycles as shown in Figure 4.14. As shown in the figure, the capacitance changed only little after 10000 cycles so it can be estimated that considerably longer cycle life is feasible.

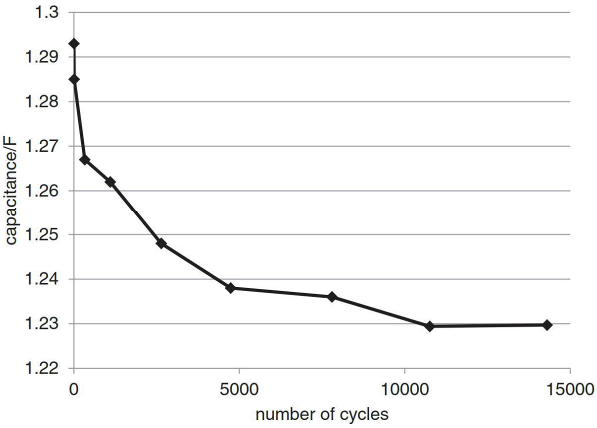

FIGURE 4.14. Capacitance of supercapacitor with asymmetric activated carbon and Ppy electrodes. Adapted from **II**.

4.4 Fabrication of monolithic supercapacitors

4.4.1 Advantages and processing

To make the fabrication of supercapacitors easier by solution processing, a novel method utilizing layers which are applied on top of each other was developed. This method eliminates the need of assembling two separate electrodes face-to-face with a separator and simultaneously adding the electrolyte.

The monolithic structure (Figure 3.1 b) sets some requirements for the current collector, electrolyte and separator materials. They should be compatible with the process parameters demanded by the layers that are to be made above them. The porosity of the activated carbon electrodes and the separator may also be challenging, since the materials to be applied onto them should not penetrate too deep to the pores. For instance activated carbon ink penetrating through the separator would result in a short-circuit between the electrodes. In the same way the upper current collector ink could destroy the porosity of the upper electrode.

The material combinations tested are shown in Table 4.3. Sample A was made to test if the concept is feasible. In this case the separator was still made of paper but the sample proved that in principle it is possible to apply the upper electrode on porous surface and further to fabricate the upper current collector on top of the electrode. The next change was to replace the paper separator with chitosan solution. The concentration of chitosan in the solution was chosen to be high enough to increase the viscosity. Thus the solution would not get that easily impregnated into the lower electrode. The experiment was done using both PET (sample B, shown in Figure 4.3 b) and PET/Al substrate (sample C). Due to the shrinkage of chitosan when cured at 95 ^{o}C, talc was added to the chitosan to aid in maintaining the dimensions during curing (sample D). The samples A-D were sealed with a cap made of the same material as the substrate. To demonstrate that it is possible to make the whole structure from solution processable materials, sample E was encapsulated with epoxy. Sample F was a normal face-to-face assembled supercapacitor and it was used as a reference.

Table 4.3. Materials used in monolithic supercapacitor experiments. Adapted from **IV**.

Sample	**Substrate**	**Separator**	**Cap**	**Structure**
A	PET/Al	2-fold paper	PET/Al	Layer-by-layer
B	PET	Chitosan	PET	Layer-by-layer
C	PET/Al	Chitosan	PET/Al	Layer-by-layer
D	PET/Al	Chitosan+talc	PET/Al	Layer-by-layer
E	PET/Al	Chitosan	Epoxy	Layer-by-layer, Monolithic
F (reference)	PET/Al	Paper	NA	Face-to-face assembled

Figure 4.15 shows the cross-section of a monolithic supercapacitor structure. The substrate is on the left. The structure includes lower current collector (20 µm), lower electrode (70 µm), chitosan separator (20 µm), upper electrode (100 µm) and upper current collector (15 µm).

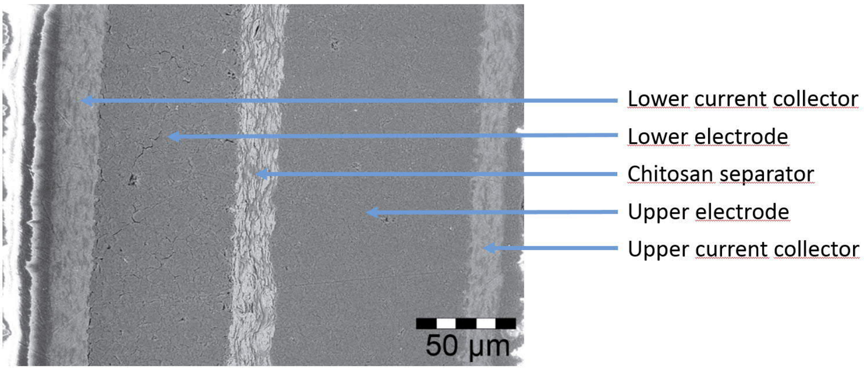

FIGURE 4.15. Cross-section of a monolithic supercapacitor structure. Adapted from **IV**.

4.4.2 Electrical properties

In principle, the structure of the monolithic supercapacitors is electrically similar to the structure used in face-to-face assembled supercapacitors. The area and thickness of the electrodes is comparable with many of the face-to-face assembled supercapacitors (**III**). Thus it is expected that the capacitance values are approximately similar. The capacitance values of samples A-F were 0.26-0.43 F.

A difference that could possibly change electrical properties is the use of chitosan separator instead of paper. The ionic resistance of the chitosan separator soaked with aqueous NaCl solution was defined to be 0.8 Ωm (**IV**). Thus for the geometry used in the tested supercapacitors (dry thickness 20 µm and area 2.4 cm^2), the resistance caused by the separator is 0.17 Ω. When compared to the total ESR value of 12-32 Ω measured for the monolithic supercapacitors, it can estimated that the change in separator material does not remarkably increase the ESR.

Figure 4.16 shows the results of galvanostatic charge/discharge measurements and cyclic voltammetry for samples A, D, E and F. The differences between the samples are to a great extent caused by ESR variations. With 1 mA current the charge-discharge curves still look quite similar to each other, but with 10 mA the IR drop gets bigger indicating higher ESR especially in sample E. The shape of the CV loop also changes with the increase of ESR causing transformation from the rectangular shape for an ideal supercapacitor with no ESR. Since the ESR is mainly caused by the current collectors, graphite ink thickness variations can cause significant differences. Beside other uncertainties in the manufacturing process, the origin of the variations is largely the warping of the substrate due to dimensional changes in the chitosan separator during curing.

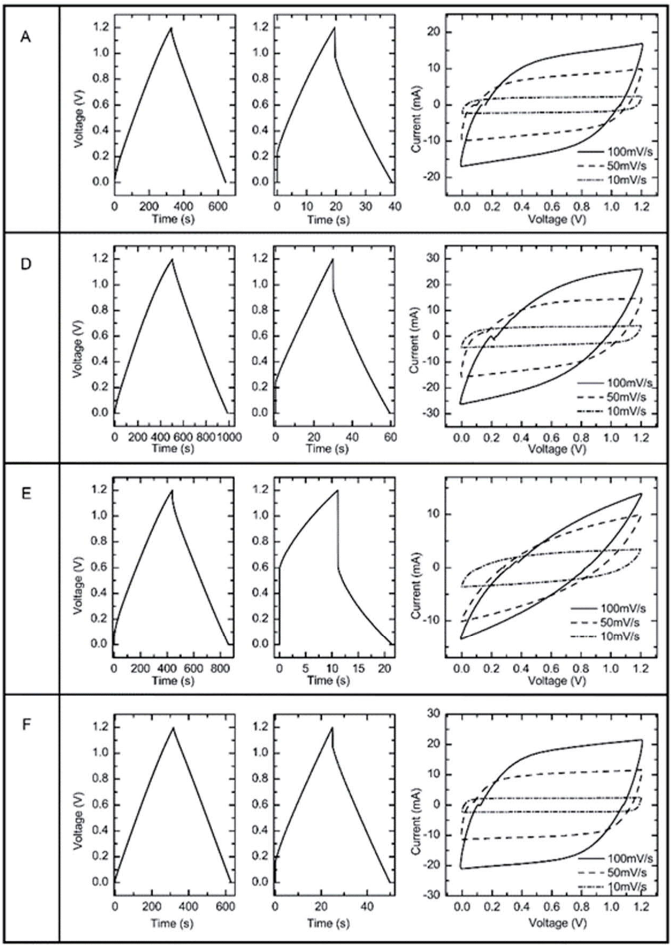

Figure 4.16. Constant current (1 mA and 10 mA) charge-discharge curves and cyclic voltammetry measurements. Sample codes on the left refer to Table 4.3. Adapted from **IV**.

5 Conclusions

In this study various supercapacitor structures were developed and characterized. The capacitance of the supercapacitors made was of the order of 0.1-1 F. The devices are intended to be applied as energy storage components either to provide power for system when the primary energy source such as light is not available or to facilitate momentary higher power output. This kind of supercapacitors can be used in Internet of Things applications to facilitate wireless sensor systems including energy storage without batteries.

The work was guided by the demand to avoid toxic and harmful materials. To ensure the feasibility of the supercapacitors in numerous applications, the use of inexpensive materials was preferred. To keep the manufacturing costs low, the materials and structures were chosen to facilitate the use of printing methods in the fabrication process. To make R2R manufacturing possible, the flexibility of the substrates, current collectors and electrodes is essential. Due to the flexibility also the devices are bendable which widens the application range.

Various substrate materials were compared with each other. Polymer coated paperboard, polymer films and polymer-metal laminates were found to be feasible alternatives. The requirements set *e.g.* for lifetime determine the choice between these. Especially barrier properties to prevent electrolyte evaporation are critical from this point of view. Aluminum foil provided good barrier properties resulting in very low evaporation rate. The lifetime was estimated both by measuring the mass change of the supercapacitors to define the evaporation rate and cycle life by making continuous charge-discharge cycles. Based on the evaporation rate the lifetime would be several years. The cycle life of up to 40000 cycles was proved but after this test the devices were still functional having 91 % of the original capacitance remaining. Thus the research proved the feasibility of these supercapacitors also when relatively long lifetime is required.

Based on comparing different substrate materials it seems probable that improved barrier properties are essential also in decreasing the self-discharge rate of the supercapacitors since oxygen penetration from air to the electrolyte is a potential reason for self-discharge. The self-discharge and leakage current measurements suggest that with aluminum barrier these properties can be improved. When charged to 1.2 V and maintained at this voltage for 24 hours the self-discharge resulted in voltage decrease to about 0.9 V in 30 days. The low self-discharge makes it possible to use the supercapacitors even in applications where the time period between consecutive supercapacitor chargings is several days.

The equivalent series resistance of the supercapacitors varied from values below 1 Ω to above 30 Ω. The highest resistance values were measured for devices with graphite ink alone as current collector. The resistance of graphite ink current collectors can be decreased by making them shorter, wider and thicker. However, with metallic current collectors such as silver ink or aluminum foil the decrease in resistance is considerably larger. Typically for the supercapacitor layout used in this work the ESR for devices with metallic current collectors was of the order of 1 Ω and for the devices with graphite ink current collectors of the order of 10 Ω. The requirement of maximum voltage drop due to ESR defines the maximum acceptable ESR level. In case 100 mV voltage loss is acceptable, with 1 Ω ESR current can be up to 100 mA. Correspondingly 10 Ω ESR would allow current level up to 10 mA.

The drawback of metallic current collectors with aqueous electrolyte is the possibility of corrosion in case the electrolyte can reach the metallic current collector surface. Graphite ink applied on top of the metallic current collector can inhibit the contact between the electrolyte and metal surface, but it was found that in practice the graphite ink is not dense enough to fully isolate the materials.

The electrode materials used were activated carbon and polypyrrole. In the activated carbon ink used as electrodes, chitosan was used as a binder. Compared with conventional supercapacitor electrodes with polymer binders containing fluorine, the chitosan alternative can be considered as an environmentally benign alternative. It also facilitated the solution processing of the electrodes using only water based solvent thus avoiding the need to use harmful or toxic organic solvents. Polypyrrole electrodes were tested in various configurations. They resulted in approximately twice as high specific capacitance as the values obtained with activated carbon. A symmetric supercapacitor with polypyrrole electrodes had poor cycle life, but an asymmetric device with one electrode made of polypyrrole and one of activated carbon showed considerably longer lifetime with about 95 % of the original capacitance remaining still after 14300 charge-discharge cycles.

To facilitate easy manufacturing of supercapacitors by solution processing, a method to prepare them monolithically was developed. The ink layers were applied on top of each other. At first basically a normal electrode structure with graphite ink current collector and activated carbon electrode was fabricated. Then a chitosan layer to act as separator was applied to cover the electrode. On the chitosan layer an activated carbon electrode layer was applied and further another current collector layer. Aqueous electrolyte impregnating to porous electrodes and chitosan was added and the structure was sealed either with polymer foil, polymer-aluminum laminate or epoxy. The electrical properties of the monolithic supercapacitor were comparable with the supercapacitors made by assembling two separate electrodes face-to-face thus proving the feasibility of the structure.

The target to develop flexible and small supercapacitors for e.g. Internet of Things or wireless sensor network applications was met in this study. A further goal was to use environmentally benign non-toxic materials in order to enable disposable or incinerable devices. The research work proved that the supercapacitors can be fabricated by using inexpensive and environmentally friendly materials by applying scalable solution based processes thus making large-scale production feasible.

6 References

Abbas, Q., Pajak, D., Frackowiak, E. & Béguin, F. (2014). Effect of binder on the performance of carbon/carbon symmetric capacitors in salt aqueous electrolyte, Electrochimica Acta, Vol. 140, pp. 132–138.

Abbas, Q., Ratajczak, P., Babuchowska, P., Le Comte, A., Bélanger, D., Brousse, T. & Béguin, F. (2015). Strategies to improve the performance of carbon/carbon capacitors in salt aqueous electrolytes, Journal of Electrochemical Society, Vol. 162, pp. A5148-A5157.

Abbas, Q., Babuchowska, P., Frackowiak, E. & Béguin, F. (2016). Sustainable AC/AC hybrid electrochemical capacitors in aqueous electrolyte approaching the performance of organic systems, Journal of Power Sources Vol. 326, pp. 652-659.

Akinyele, D. & Rayudu, R. (2014). Review of energy storage technologies for sustainable power networks, Sustainable Energy Technologies and Assessments, Vol. 8, pp. 74–91.

Alonso, M. & Finn, E. (1979). Fundamental University Physics. Volume II. Fields and Waves, Addison-Wesley Publishing Company, Reading, Massachusetts, USA, 528 p.

Andreas, H. (2015). Self-Discharge in Electrochemical Capacitors: A Perspective Article, Journal of Electrochemical Society, Vol. 162, pp. A5047-A5053.

Aslan, M., Weingarth, D., Herbeck-Engel, P., Grobelsek, I. & Presser, V. (2015). Polyvinylpyrrolidone/polyvinyl butyral composite as a stable binder for castable supercapacitor electrodes in aqueous electrolytes, Journal of Power Sources, Vol. 279, pp. 323-333.

Azaïs, P., Duclaux, L., Florian, P., Massiot, D., Lillo-Rodenas, M., Linares-Solano, A., Peres, J.,Jehoulet, C. & Béguin, F. (2007). Causes of supercapacitors ageing in organic electrolyte, Journal of Power Sources, Vol. 171, pp. 1046–1053.

Azaïs, P. (2013). Manufacturing of Industrial Supercapacitors, in: Béguin, F. & Frackowiak, E. (ed.), Supercapacitors: Materials, Systems and Applications, Wiley-VCH, Germany, pp. 307-371.

Balducci, A. & Schütter, C. (2015) Carbon blacks as active materials for electrochemical double layer capacitors, BOLETIN del Grupo Español del Carbón, no 37 (September), pp. 2-5.

Barbieri, O., Hahn, M., Herzog, A. & Kötz, R. (2005). Capacitance limits of high surface area activated carbons for double layer capacitors, Carbon Vol. 43, pp. 1303–1310.

Béguin, F. & Frackowiak, E. (2013). Preface, in: Béguin, F. & Frackowiak, E. (ed.), Supercapacitors: Materials, Systems and Applications, Wiley-VCH, Germany, pp. XIX-XX.

Blomquist, N., Wells, T., Andres, B., Bäckström, J., Forsberg, S. & Olin, H. (2017). Metal-free supercapacitor with aqueous electrolyte and low-cost carbon materials, Scientific Reports, Vol. 7, 39836; doi: 10.1038/srep39836, pp. 1-7.

Bohlen, O., Kowal, J. & Sauer, D. (2007). Ageing behaviour of electrochemical double layer capacitors: Part I. Experimental study and ageing model, Journal of Power Sources, Vol. 172, pp. 468–475.

Bohlen, O., Kowal, J. & Sauer, D. (2007). Ageing behaviour of electrochemical double layer capacitors: Part II. Lifetime simulation model for dynamic applications, Journal of Power Sources, Vol. 173, pp. 626-632.

Brousse, T., Bélanger, D. & Guay, D. (2013). Asymmetric and Hybrid Devices in Aqueous Electrolytes, in: Béguin, F. & Frackowiak, E. (ed.), Supercapacitors: Materials, Systems and Applications, Wiley-VCH, Germany, pp. 257-288.

Bryan, A., Santino, L., Lu, Y., Acharya, S. & D´Arcy, J. (2016). Conducting Polymers for Pseudocapacitive Energy Storage, Chemistry of Materials, Vol. 28, pp. 5989-5998.

Bussmann, web page. Available (accessed 29.6.2018):
http://www.cooperindustries.com/content/public/en/bussmann/electronics/products/eaton-supercapacitors.html

Buykens, A. (2013). Incineration Technologies, Springer, New York, USA, 89 p.

Chmiola, J., Yushin, G., Gogotsi, Y., Portet, C., Simon, P. & Taberna, P. (2006). Anomalous increase in carbon capacitance at pore size below 1 nm. Science, Vol. 313, pp. 1760–1763.

Choudhury, N., Northrop, P., Crothers, A., Jain, S. & Subramanian, V. (2012). Chitosan hydrogel-based electrode binder and electrolyte membrane for EDLCs: experimental studies and model validation, Journal of Applied Electrochemistry, Vol. 42, pp. 935–943.

Conway, B., Pell, W. & Liu, T. (1997). Diagnostic analyses for mechanisms of self-discharge of electrochemical capacitors and batteries, Journal of Power Source, Vol. 65, pp. 53-59.

Conway, B. (1999). Electrochemical Supercapacitors, Scientific Fundamentals and Technological Applications, Springer, New York, USA, 736 p.

Demarconnay, L., Raymundo-Piñero, E. & Béguin, F. (2010). A symmetric carbon/carbon supercapacitor operating at 1.6 V by using a neutral aqueous solution, Electrochemistry Communications, Vol. 12, pp. 1275–1278.

Edberg, J., Inganäs, O., Engquist, I. & Berggren M. (2018). Boosting the capacity of all-organic paper supercapacitors using wood derivatives, Journal of Materials Chemistry A, Vol. 6, pp. 145-152.

Electrodag PF 407C Technical Data Sheet (2012). Acheson, 2 p. Available (accessed 2.3.2018):
https://tds.us.henkel.com/NA/UT/HNAUTTDS.nsf/web/4152E6E550368950852576230071689A/$File/ELECTRODAG%20PF-407C-EN.pdf

Electrodag PF 410 Produktdatenblatt. Acheson Colloiden, 2 p. Available (accessed 2.3.2018): http://www.silitech.ch/upload/fiche_technique_D/304.PDF

Endo, M., Strano, M. & Ajayan, P. (2008). Potential Applications of Carbon Nanotubes, in: Jorio, A., Dresselhaus, G. & Dresselhaus M. (ed.), Carbon Nanotubes, Advanced Topics in the Synthesis, Structure, Properties and Applications, Springer, Topics in Applied Physics, Vol. 111, Berlin, Germany, pp. 13-61.

Engineering Toolbox, web page. Available (accessed 2.3.2018): https://www.engineeringtoolbox.com/resistance-resisitivity-d_1382.html

Fic, K., Lota, G., Meller, M. & Frackowiak, E. (2012). Novel insight into neutral medium as electrolyte for high-voltage supercapacitors, Energy & Environmental Science, Vol. 5, pp. 5842-5850.

Frackowiak, E. Abbas, Q. & Béguin, F. (2013). Carbon/carbon supercapacitors, Journal of Energy Chemistry, Vol. 22, pp. 226–240.

Ganz, S., Sauer, H., Weissenseel, S., Zembron, J., Tone, R., Dörsam, E., Schaefer, M. & Schulz-Ruthenberg, M. (2016). Printing and Processing Techniques, in: Nisato, G., Lupo, D. & Ganz S. (ed.), Organic and Printed Electronics Fundamentals and Applications, Pan Stanford Publishing, Singapore, pp. 47-116.

González, A., Goikolea, E., Barrena, J. & Mysyk, R. (2016). Review on supercapacitors: Technologies and materials, Renewable and Sustainable Energy Reviews, Vol. 58, pp. 1189–1206.

Hahn, M., Furrer, P., Schnuder, B., Bärtsch R., Kötz, R., Haas, O., Ohler, C. & Carlen, M. (2000). Double-Layer Capacitors Based on Glassy Carbon and Sulfuric Acid – Mechanisms of Self Discharge, 10th International Seminar on Double Layer Capacitors and Similar Energy Storage Devices, Deerfield Beach, Florida, USA, December 4-6, 2000, Florida Educational Seminars, Inc., pp 1-12.

He, M., Fic, K., Frackowiak, E., Novák, P., & Berg, E. (2016). Ageing phenomena in high-voltage aqueous supercapacitors investigated by in situ gas analysis, Energy & Environmental Science, Vol. 9, pp. 623-633.

Hösel, M. (2013). Large-scale Roll-to-Roll Fabrication of Organic Solar Cells for Energy Production, Ph.D. Thesis, Technical University of Danmark, 120 p. Available: http://orbit.dtu.dk/files/89079576/phdthesis_markushoesel_final_online.pdf.

IEC 62391-1 (2006). International Standard: Fixed electric double-layer capacitors for use in electronic equipment – Part 1: Generic specification, International Electrotechnical Commission, Geneva, 31 p.

Ioxus, web page. Available (accessed 29.6.2018):
http://www.ioxus.com/english/products/technology/

Jiménez-Cordero, D., Heras, F., Gilarranz, M. & Raymundo-Piñero, E. (2014). Grape seed carbons for studying the influence of texture on supercapacitor behaviour in aqueous electrolytes, Carbon, Vol. 71, pp. 127 –138.

Keskinen, J., Jansson, E., von Hertzen, L., Yli-Rantala, E., Maaninen, T., Jussila, S., Johansson, M., Remonen, T., Pettersson, F., Kielosto, S., Eiroma, K., Flyktman, T., Grönberg, V., Zhang, Y., Ranta, A., Wilén, C., Österbacka, R., Kauranen, P., Munter, T. & Tappura, K. (2014). Printed supercapacitors Project report, VTT-R-02902-14, VTT, Tampere, 66 p. Available: http://www.vtt.fi/inf/julkaisut/muut/2014/VTT-R-02902-14.pdf

Kim, B., Hong, J., Wallace, G. & Park, H. (2015). Recent Progress in Flexible Electrochemical Capacitors: Electrode Materials, Device Configuration, and Functions, Advanced Energy Materials, Vol. 5, 1500959, pp. 1-33.

Kouchachvili, L., Maffei, N. & Entchev, E. (2014) .Novel binding material for supercapacitor electrodes, Journal of Solid State Electrochemistry, Vol. 18, pp.2539–2547.

Kuraray Activated Carbon for Supercapacitors, Kuraray Chemical Co, web page (accessed 20.12.2017): http://www.kuraraychemical.com/products/sc/capacitor.htm.

Kötz, & Carlen, M. (2000). Principles and applications of electrochemical capacitors, Electrochimica Acta, Vol. 35, pp. 2483-2498.

Kötz, R., Hahn, M. & Gallay, R. (2006).Temperature behavior and impedance fundamentals of supercapacitors, Journal of Power Sources, Vol. 154, pp. 550–555.

Lawrence, D., Kohler, J., Brollier, B., Claypole, T. & Burgin, T. (2004). Manufacturing Platforms of Printing Organic Circuits, in: Gamota, D., Brazis, P., Kalyanasundaram, K. & J. Zhang (ed.), Printed organic and molecular electronics, Kluwer Academic Publishers, USA, pp. 161-346.

Lehtimäki, S. (2017). Printed Supercapacitors for Energy Harvesting Applications, Tampere University of Technology, Publication 1463, 46 p. Available: https://tutcris.tut.fi/portal/files/10141460/lehtim_ki_1463.pdf

Lehtimäki, S., Li, M., Salomaa, J., Pörhönen, J., Kalanti, A., Tuukkanen, S., Heljo, P., Halonen, K. & Lupo, D. (2014). Performance of printable supercapacitors in an RF energy harvesting circuit, Electrical Power and Energy Systems, Vol. 58, pp. 42–46.

Lehtimäki, S., Railanmaa, A., Keskinen, J., Kujala, M., Tuukkanen, S. & Lupo, D. (2017). Performance, stability and operation voltage optimization of screen-printed aqueous supercapacitors, Scientific Reports, Vol. 7, 46001, pp. 1-9.

Li, Q., Jiang, R., Dou, Y., Wu, Z., Huang, T., Feng, D., Yang, J., Yu, A. & Zhao, D. (2011). Synthesis of mesoporous carbon spheres with a hierarchical pore structure for the electrochemical double-layer capacitor, Carbon, Vol. 49, pp. 1248-1257.

LS Mtron, web page. Available (accessed 29.6.2018):
http://www.lsmtron.com/page/popup/productAllView.asp?divisionCode=D0700

Luo, X., Wang, J., Dooner, M. & Clarke, J. (2015), Overview of current development in electrical energy storage technologies and the application potential in power system operation, Applied Energy, Vol. 137, pp. 511−536.

Macfarlane, D., Tachikawa, N., Forsyth, M., Pringle, J. Howlett, P., Elliott,G., Davis, J., Watanabe, M., Simon, P. & Angell, C. (2014), Energy applications of ionic liquid, . Energy & Environmental Science, Vol. 7, pp. 232-250.

MacLeod, D. (2007). Wire-Wound Rod Coating, in: Tracton, A. (ed.) Coatings Technology, Fundamentals, Testing and Processing Techniques, CRC Press, Florida, USA, pp.19-1 – 19-8.

Marsh, H. & Rodríguez-Reinoso, F. (2006). Activated Carbon, Elsevier Science, Oxford, UK, 554 p.

Maxwell, web page. Available (accessed 29.6.2018):
http://www.maxwell.com/products/ultracapacitors/cells

McDougall, G. (1991). The physical nature and manufacture of activated carbon, Journal of the Southern African Institute of Mining and Metallurgy, Vol. 91(4), pp. 109-120.

Murata, web page. Available (accessed 29.6.2018):
https://www.murata.com/products/capacitor/edlc

Niu, J., Conway, B. & Pell, W. (2004). Comparative studies of self-discharge by potential decay and float-current measurements at C double-layer capacitor and battery electrodes, Journal of Power Sources, Vol. 135, pp. 332–343.

Nippon Chemi-Con, web page. Available (accessed 29.6.2018): http://www.chemi-con.co.jp/e/catalog/dl.html

Obreja, V. (2014). Supercapacitors Specialities – Materials Review, AIP Conference Proceedings, Vol. 1597, pp.98-120.

Panasonic, web page. Available (accessed 29.6.2018):
https://industrial.panasonic.com/ww/products/capacitors/edlc

Pandolfo, A. & Hollenkamp, A. (2006). Carbon properties and their role in supercapacitors, Journal of Power Sources, Vol. 157, pp. 11–27.

Pandolfo T., Ruiz, V., Sivakkumar, S. & Nerkar, J. (2013). General Properties of Electrochemical Capacitors, in: Béguin, F. & Frackowiak, E. (ed.), Supercapacitors: Materials, Systems and Applications, Wiley-VCH, Germany, pp. 69-109.

Pörhönen, J., Rajala, S., Lehtimäki, S. & Tuukkanen, S. (2014). Flexible Piezoelectric Energy Harvesting Circuit with Printable Supercapacitor and Diodes, IEEE Transactions on Electron Devices, Vol. 61, pp. 3303-3308.

Ratajczak, P., Jurewicz, K. & Béguin, F. (2014). Factors contributing to ageing of high voltage carbon/carbon supercapacitors in salt aqueous electrolyte, Journal of Applied Electrochemistry, Vol. 44, pp. 475–480.

Rodriguez-Reinoso, F. (1998). The role of carbon materials in heterogeneous catalysis, Carbon, Vol. 36, pp. 159-175.

Roselli, L., Mariotti, C., Mezzanotte, P., Alimenti, F., Orecchini, G., Virili, M. & Carvalho, N. (2015). Review of the present technologies concurrently contributing to the implementation of the Internet of Things (IoT) paradigm: RFID, Green Electronics, WPT and Energy Harvesting, IEEE Topical Conference on Wireless Sensors and Sensor Networks (WiSNet), San Diego, California, USA, January 25-28, 2015, IEEE, pp.1-3.

Ruiz, V., Blanco, C., Granda, M., Menéndez, R. & Santamaría, R. (2007). Influence of electrode preparation on the electrochemical behaviour of carbon-based supercapacitors, Journal of Applied Electrochemistry, Vol. 37, pp. 717–721.

Sabihuddin, S., Kiprakis, A. & Mueller, M. (2015). A Numerical and Graphical Review of Energy Storage Technologies, Energies, Vol. 8, pp. 172-216.

Senich, G. & Florin, R. (1983). Radiation curing of inks and coatings, NBSIR 82-2722, U.S. Department of Commerce, Washington DC, USA, 128 p.

Sevilla, M. & Mokaya, R. (2014). Energy storage applications of activated carbons: supercapacitors and hydrogen storage, Energy & Environmental Science, Vol. 7, pp. 1250-1280.

Shaikh, F. & Zeadally, S. (2016). Energy harvesting in wireless sensor networks: A comprehensive review, Renewable and Sustainable Energy Reviews, Vol. 55, pp. 1041–1054.

Simon, P. & Gogotsi, Y. (2008). Materials for electrochemical capacitors, Nature Materials, Vol. 7, pp. 845-854.

Simon, P., Taberna, P. & Béguin, F. (2013). Electrical Double-Layer Capacitors and Carbons for EDLCs, in: Béguin, F. & Frackowiak, E. (ed.), Supercapacitors: Materials, Systems and Applications, Wiley-VCH, Germany, pp. 131-165.

Simon, P., Gogotsi, Y. & Dunn, B. (2014). Where Do Batteries End and Supercapacitors Begin?, Science, Vol. 343, pp. 1210-1211.

Singh, A. & Chandra, A. (2015). Significant Performance Enhancement in Asymmetric Supercapacitors based on Metal Oxides, Carbon nanotubes and Neutral Aqueous Electrolyte, Scientific Reports, Vol. 5:15551, pp. 1-12.

Smith, P., Tran, T., Jiang, T. & Chung, J. (2013). Lithium-ion capacitors: Electrochemical performance and thermal behavior, Journal of Power Sources, Vol. 243, pp. 982-992.

Snook, G., Kao, P. & Best, A. (2011). Conducting-polymer-based supercapacitor devices and electrodes, Journal of Power Sources, Vol. 196, pp. 1–12.

Suganuma, K. (2014). Introduction to Printed Electronics, Springer, New York, USA, 148 p.

Vangari, M., Pryor, T. & Jiang, L. (2013). Supercapacitors: Review of Materials and Fabrication Methods, Journal of Energy Engineering, Vol. 139, pp. 72-79

Varzi, A. & Passerini, S. (2015). Enabling high areal capacitance in electrochemical double layer capacitors by means of the environmentally friendly starch binder, Journal of Power Sources, Vol. 300, pp. 216-222.

Varzi, A., Raccichini, R., Marinaro, M. Wohlfahrt-Mehrens, M. & Passerini, S. (2016). Probing the characteristics of casein as green binder for non-aqueous electrochemical double layer capacitors' electrodes, Journal of Power Sources, Vol. 326, pp. 672-679.

Veit, H. & Bernandes, A. (ed.) (2013). Electronic Waste. Recycling Techniques, Springer, Cham, Switzerland, 158 p.

Wang, G., Zhang, L., & Zhang, J. (2012). A review of electrode materials for electrochemical supercapacitors, Chemical Society Reviews, Vol. 41, pp. 797–828.

Wang, S., Liu, N., Yang, C., Liu, W., Su, J., Li, L., Yang, C. & Gao, Y. (2015). Fully screen printed highly conductive electrodes on various flexible substrates for asymmetric supercapacitors, RSC Advances, Vol. 5, pp. 85799-85805.

Wang, Z., Zhang, W., Li, X. & Gao, L. (2016). Recent progress in flexible energy storage materials for lithium-ion batteries and electrochemical capacitors: A review, Journal of Materials Research, Vol 31, pp. 1648-1664.

Weinstein, L. & Dash, R. (2013). Supercapacitor carbons. Have exotic carbons failed?, Materials Today, Vol. 16, pp. 356-357.

Wengeler, L., Schmitt, M., Peters, K., Scharfer, P. & Schabel, W. (2013). Comparison of large scale coating techniques for organic and hybrid films in polymer based solar cells, Chemical Engineering and Processing, Vol. 68, pp. 38– 44.

White, R. (2015). The Search for Functional Porous Carbons from Sustainable Precursors, in: White, R. (ed.), Porous Carbon Materials from Sustainable Precursors, Royal Society of Chemistry, Cambridge, United Kingdom, pp. 3-49.

Winter, M. & Brodd, R. (2004). What Are Batteries, Fuel Cells, and Supercapacitors?, Chemical Reviews, Vol. 104, pp. 4245−4269.

Wolf, A, Brown, M. & Prentiss, P. (1985). Concentrative properties of aqueous solutions: conversion tables, in: Weast, R. (ed.), CRC Handbook of Chemistry and Physics, CRC Press, Boca Raton, Florida, USA, pp. D223-D272.

Worrell, E. & Reuter, M. (ed.) (2014). Handbook of Recycling. State-of-the-Art for Practitioners, Analysts, and Scientists, Elsevier, Amsterdam, Netherlands, 589 p.

Xiong, G., Kundu, A. & Fisher, T. (2015). Thermal Effects in Supercapacitors, SpringerBriefs in Thermal Engineering and Applied Science, Springer, New York, USA, 147 p.

Yan, J., Wang, Q., Wei, T. & Fan, Z. (2014). Recent Advances in Design and Fabrication of Electrochemical Supercapacitors with High Energy Densities, Advanced Energy Materials, Vol. 4:1300816, pp. 1-43.

Yu, A., Chabot, V. & Zhang, J. (2013). Electrochemical Supercapacitors for Energy Storage and Delivery, Fundamentals and Applications, CRC Press, Boca Raton, Florida, USA, 2013, 355 p.

Zhang, L. & Zhao, X. (2009). Carbon-based materials as supercapacitor electrodes, Chemical Society Reviews, Vol. 38, pp. 2520-2531.

Zhong, C., Deng, Y., Hu, W., Qiao, J., Zhang, L. & Zhang, J. (2015). A review of electrolyte materials and compositions for electrochemical supercapacitors, Chemical Society Reviews, Vol. 44, pp. 7484-7539.

Zhong, C., Deng, Y., Hu, W., Qiao, J. & Zhang J. (2016). Fundamentals of Electrochemical Supercapacitors, in: Zhong, C., Deng, Y., Hu, W., Sun, D., Han, X., Qiao, J. & Zhang J.(ed.), Electrolytes for Electrochemical Supercapacitors, CRC Press 2016, Boca Raton, Florida, USA, pp. 1-29.

Tampereen teknillinen yliopisto
PL 527
33101 Tampere

Tampere University of Technology
P.O.B. 527
FI-33101 Tampere, Finland

ISBN 978-952-15-4180-3
ISSN 1459-2045